AN EXPERIMENTAL STUDY OF CENTRALLY LOADED X-SHAPED COLUMNS

A Thesis
Presented to
the Faculty of the Department of Civil Engineering
The University of Houston

In Partial Fulfillment
of the Requirements for the Degree
Master of Science in Civil Engineering

---

by

Sung Joo Lim

August, 1969

ACKNOWLEDGEMENTS

The author wishes to express his deepest gratitude to Dr. William Graff for serving as Chairman of the Committee and providing indispensable guidance throughout the development of the project.

Sincere appreciation is due Dr. Ardis White for his help and encouragement during the experimental work and his constant guidance, without which the project might well not have been completed.

To Professor David Red, an expression of indebtedness is due, for raising the basic problems of this project, and providing the column specimens.

This thesis was typed by Mrs. Marjorie Carroll, who deserves special acknowledgement for "a difficult job well done."

DEDICATION

I would like to dedicate this thesis to my mother and brothers, still in Korea, and especially to my wife, for their encouragement and faith.

AN EXPERIMENTAL STUDY OF CENTRALLY
LOADED X-SHAPED COLUMNS

An Abstract of a Thesis
Presented to
the Faculty of the Department of Civil Engineering
The University of Houston

In Partial Fulfillment
of the Requirements for the Degree
Master of Science in Civil Engineering

---

by
Sung Joo Lim
August, 1969

ABSTRACT

The column strengths of the X-shaped cross section are analyzed theoretically and experimentally. In theoretical analyses, the Euler load in the elastic range and Bleich's modification in the inelastic range are considered for the upper limit and the AISC column formulas are taken as the lower limit of the column strength. The column strengths in between the upper and lower bounds are calculated and drawn in on the curves. The calculations take into consideration the accidental end eccentricities and the shape factors as suggested by F. Bleich. The experimental data obtained from the four primary tests are shown as verification of the theoretical calculations and the X-shaped columns are considered to be strong enough to serve as structural members.

TABLE OF CONTENTS

CHAPTER PAGE

LIST OF TABLES

LIST OF FIGURES

CHAPTER I

INTRODUCTION

The two important things for an engineer to take into consideration in the design of columns are stability and economy. There are, of course, factors other than these; such as appearance, serviceability, durability, and cost of maintenance.[1]

The shape of the strongest column was studied rationally by J. B. Keller as "an equilateral triangle as cross section, and it is tapered along its length, being thickest in the middle and thinnest at its ends."[2] However, studying the strongest column is not the concern of this thesis.

The X-shaped column was devised by Professor David Red in the Architectural Department of the University of Houston, taking into account the appearance and easy connection with other structural members. The question was raised by him whether this newly devised X-shaped column has as much strength as other widely used column shapes, and whether this X-shaped column is serviceable in the field.

The thesis is written to answer these questions.

Figure 1 shows a standard 12WF72 cross section compared with the X-shaped section with slightly less area. With the area, material, and length of the column prescribed, column strength can be increased by the proper increase of the moment

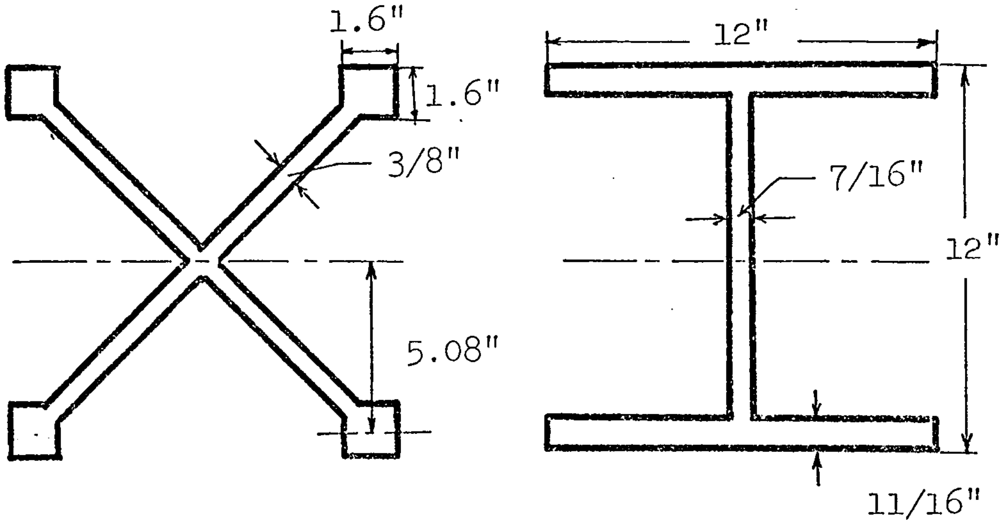

AREA: 19.24 sq. inch.

X-Shaped Column

AREA: 21.16 sq. inch.

12WF72

FIGURE 1

A NEW X-SHAPED COLUMN COMPARED WITH 12WF72 of inertia of the cross-section according to the fundamental buckling load formula, $P_{cr} = \pi^2 EI/L^2$. The rectangular bars of the X-shaped cross-section are designed to increase the moment of inertia as much as possible. The web thickness of X-shape should be governed by the limitation of rolling fabrication and the possibility of buckling.

The X-shaped column has an equal moment of inertia in all directions, while the wide flange shape has a much greater moment of inertia in one direction. Table I shows the comparative moment of inertia, section modulus, and the comparable weights.

TABLE I

COMPARISON BETWEEN X-SHAPED AND 12WF72 CROSS-SECTIONAL PROPERTIES

Section	I_{x-x} (in^4)	I_{y-y} (in^4)	S_x (in^3)	S_x/W (in^3/lb)	S_y (in^3)	S_y/W (in^3/lb)
12WF72	533.4	174.6	97.5	1.35	32.4	0.45
12 X	325	325	55.4	0.847	55.4	0.847

In Chapter II, the elastic, inelastic, and torsional theories of column strength are discussed. The theoretical buckling loads usually exceed the experimental values. The factors that cause the actual column strength to be less than the theoretical buckling load are described in Chapter III.

In Chapter III are discussed the various effects on theoretical column strength. The topics chosen are the residual stress effect, the accidental end eccentricity, and the shape of the cross section.

In Chapter IV, the theoretical column strengths are calculated and are presented by curves. The Euler curve in the elastic range and the Bleich curve in the inelastic range form the upper bound of the column strength, while the AISC allowable design formula curve makes the lower bound of the strength.

Experiments for the verification of the actual X-shaped column strength are described in Chapter V. The experiments are divided into two parts, i.e., the primary column tests and the secondary column tests. The primary column tests are aimed at measuring the buckling of the column, while the secondary tests are for determining the mechanical properties of the column material. The primary test data are plotted on the column strength curves.

Chapter VI contains a comparison of the X-shape column strength with that of the wide flange shape, and the conclusions are given in Chapter VII.

CHAPTER II

THEORY OF THE BASIC COLUMN STRENGTH

I. ELASTIC-INELASTIC BUCKLING LOAD

The critical load for a long slender compressed bar which is assumed to be linearly elastic, initially straight, centrally loaded, and with hinged-end boundary conditions, is:

$$Pcr = \frac{\pi^2 EI}{L^2} \tag{2.1}$$

where Pcr is known as the Euler buckling load.[3] Upon substitution of $I = Ar^2$ and division by A, the formula for the average stress at the Euler buckling load is obtained:

$$\sigma cr = \frac{\pi^2 E}{(KL/r)^2} \tag{2.2}$$

Here the factor K permits modification to other than hinged-end boundary conditions. For purely flexural buckling, KL is the length between inflection points and is known as the effective or equivalent length.

In the derivation of Equation (2.2), it was assumed that the material was linearly elastic, and Equation (2.2) is valid only so long as the stress σcr remains within the proportional limit. When the proportional limit of 30,000 psi and E = 30,000,000 psi of the structural steel are given, we find the minimum KL/r from Equation (2.2) to be about 100.

The results of the stub-column tests in this investigation of X-shaped cross-section have shown the proportional stress and Young's modulus to be: $\sigma p = 20{,}000$ psi and $E = 30{,}000{,}000$ psi. Consequently, the minimum KL/r is 120. The critical stress of the X-shaped column can be calculated by Equation (2.2) when KL/r ratio is greater than about 120.

If KL/r is less than 120 for the X-shaped column, the compressive stress reaches the proportional limit before buckling can occur and Equation (2.2) cannot be used. The column buckling in the inelastic range depends upon the tangent modulus Et corresponding to the L/r ratio, since different values of the material stiffness are given by the different tangents to the stress-strain curve.

Substitution of the tangent modulus Et for the elastic modulus E is then the only modification necessary to make the elastic buckling formulas applicable in the inelastic range:

$$\sigma cr = \frac{\pi^2 Et}{(KL/r)^2} \tag{2.3}$$

The values of Et are obtained by the slopes of the stress-strain curve at any point in the inelastic range. These values for the X-shaped column may be obtained by the stub-column tests. Timoshenko has introduced an equation for the calculation of Et in the case of materials like structural steel with a well-defined yield-point stress σy using the expression suggested by Arvo Ylinen as

$$\frac{d\sigma}{d\epsilon} = Et = E\,\frac{\sigma y - \sigma}{\sigma y - c\sigma} \tag{2.4}$$

where c = 0.96 to 0.89.[4] However, the writer prefers to use Bleich's parabolic formula with which it is possible to calculate the column strength in the inelastic range if the material is well defined. These calculations of column strength will be shown in Chapter IV.

II. TORSIONAL BUCKLING STRENGTH

Due to the open sections of the X-shaped column which possess very small torsional rigidity, the possibility of torsional buckling should be discussed.

R. Kappus has described buckling, saying that for centrally loaded columns of solid cross section or thick-walled, hollow cross section, only flexural (or Euler) buckling type is recognized, and the cross sections of thin-walled open or closed section and short column length buckle torsionally due to the less bending-resistant wall.[5] According to Kappus's statement, the centrally loaded long columns of X-shaped cross-section are predicted to buckle in the Euler buckling mode, and the shorter column lengths should fail torsionally.

Because of the double-symmetric section and the fact that the shear center and the centroid coincide for the X-section, no interaction of bending and twisting can occur, according to A. Chajes and G. Winter's research paper.[6]

The torsional buckling of the cruciform section which has four identical flanges and which is very similar to the X-shaped cross section subjected to uniform axial compression is presented in detail by S. P. Timoshenko.[7] The final equation considering each flange as a uniformly compressed plate simply supported along three sides and completely free along the fourth side is shown taking into account the influence of the length of the bar:

$$\sigma_{cr} = \left(0.456 + \frac{b^2}{L^2}\right) \frac{\pi^2}{6(1-\nu)} \frac{Gt^2}{b^2} \qquad (2.5)$$

where b = the width of the flange; L = the length of the member; = the poisson's ratio; and G = the shearing modulus $\frac{E}{2(1+\nu)}$.

Table II shows the calculated values of the torsional buckling with variation of the length. Let b = 2.6, t = 3/16, G = 12 x 10^6, and ν = 0.3 for the purpose of comparing with Euler's buckling load in Figure 2. It is estimated that torsional buckling is controlling when L/r of the column is less than 65.

TABLE II

TORSIONAL BUCKLING STRESSES OF DIFFERENT CRUCIFORM COLUMN LENGTH
(r = 1.3 in.)

KL/r	KL (in.)	σ_{cr} (ksi)	KL/r	KL (in.)	σ_{cr} (ksi)
20	15.38	71.23	75	57.69	67.33
25	19.23	69.72	80	61.54	67.29
30	23.08	68.90	85	65.38	67.26
35	26.92	68.40	90	69.23	67.23
40	30.77	68.08	95	73.09	67.22
45	34.62	67.86	100	76.92	67.20
50	38.46	67.70	105	80.77	67.18
55	42.31	67.59	110	84.62	67.17
60	46.15	67.50	115	88.46	67.16
65	50.00	67.43	120	92.31	67.15
70	53.85	67.37	125	96.15	67.14

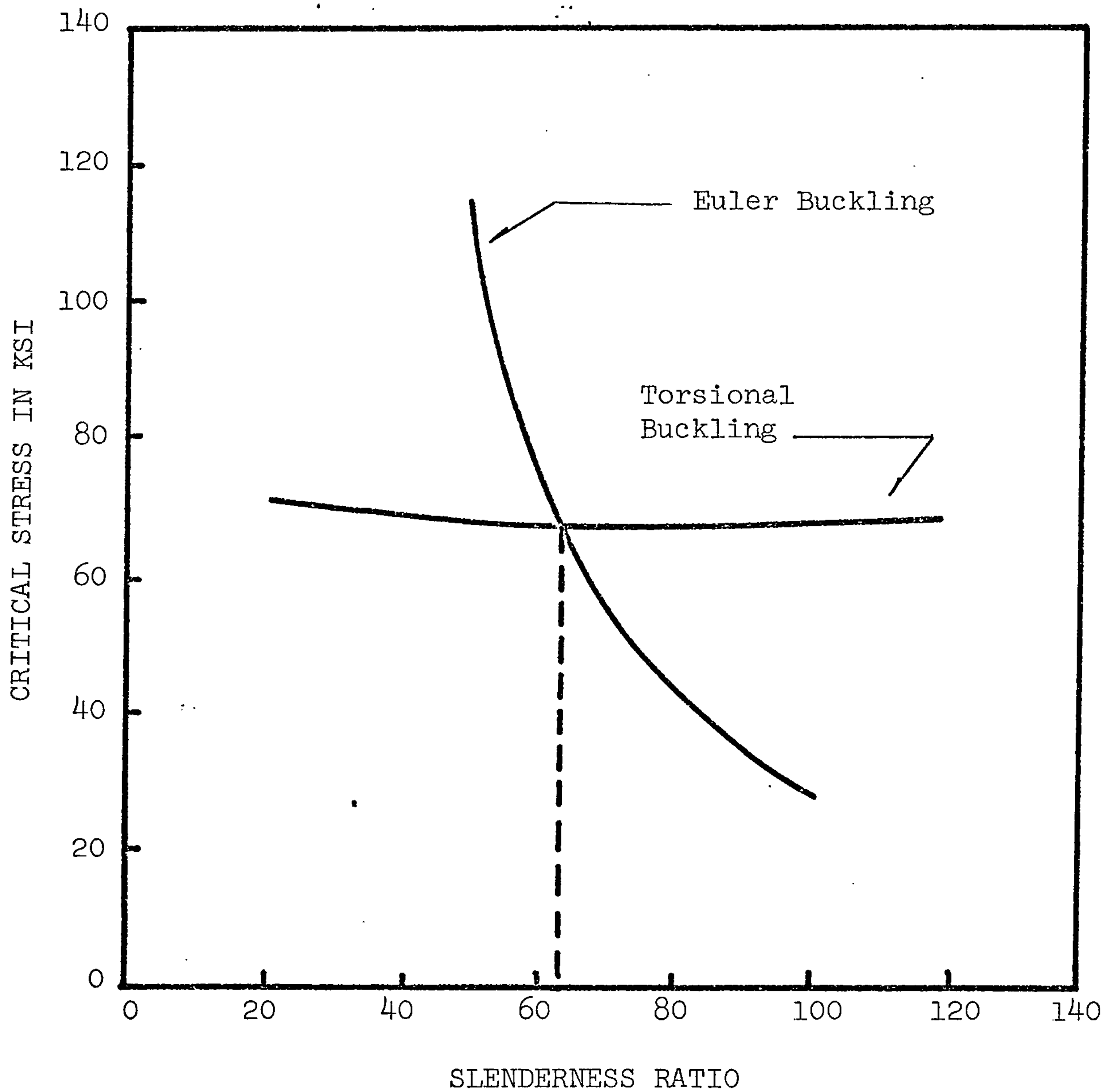

FIGURE 2

TORSIONAL BUCKLING CURVE AND EULER BUCKLING CURVE

CHAPTER III

THE EFFECTS ON COLUMN STRENGTH

The column strength discussed in the previous chapter is purely theoretical. The actual shapes of the column strength curves depend on the accuracy with which the theoretical assumptions are fulfilled.

In actual testing of the buckling of columns, the column begins to deflect before Euler's load is reached owing to various kinds of imperfection. The factors that cause actual column strength to be different from the Euler's critical load are summarized in Table III.

This chapter will cover the discussion of residual stress, accidental end eccentricity, and cross-sectional shape of the X-shaped column.

I. RESIDUAL STRESSES

Residual stresses are formed in a structural member as a result of plastic deformations. In rolled shapes, these deformations always occur during the process of cooling from the rolling temperature to air temperature.

Residual stresses also are formed as a result of fabrication operations, such as in the process of cold-bending and cambering. Residual stresses are also introduced during the welding operation as a result of the localized heat input and resultant plastic deformation.[8]

TABLE III

FACTORS THAT CAUSE ACTUAL COLUMN STRENGTH TO BE DIFFERENT FROM THE EULER CRITICAL LOAD[9]

Factors Related to Basic Properties of Material	Factors Introducing Accidental Bending Stress	Factors Related to Type or Shape of Column
1. Non-linearity in actual stress-strain relationships in compression as obtained from a small coupon test.	1. Accidental end eccentricity.	1. Shear deformation, especially in built-up columns having lacing, batten plates, etc.
2. Variation in yield strength over column cross-section.	2. Accidental curvature.	2. Local buckling, especially when post-buckling strength of thin-walled plate components is a design factor.
3. Residual stress (primary factor in structural steels).	3. Accidental lateral load, or lateral load unrelated to primary column load.	3. Torsional buckling.
4. Creep.	4. Thermal effects.	

The magnitude and distribution of residual stresses may be estimated by a stub column test. If, instead of a small coupon, a stub column section is used to determine an average stress-strain curve, the tangent modulus determined therefrom will reflect both the presence of residual stress and the variation in yield stress over the cross section.

If the material has uniform yield stress, the effective proportional limit of the stub column will be

$$\sigma_p = \sigma_y - \sigma_{rc} \tag{3.1}$$

Yielding occurs when the residual stress σ_{rc} plus the applied stress σ_p is equal to σ_y.

When more load is applied, the average stress and average strain are not proportional to one another, and a non-linear stress-strain relationship results for the section as a whole. Figure 3 shows the influence of residual stress on the stress-strain curve when the X-shaped stub column is centrally loaded.

The existence of residual stress in the cross section reduces the buckling strength, since there is an early localized yielding at certain portions of the cross section. This reduction, according to Beedle and Tall,[10] is greatest when the slenderness ratio is between 70 and 90.

II. ACCIDENTAL END ECCENTRICITY

Due to the imperfections of the settlement of the loading devices when X-shaped columns are centrally loaded,

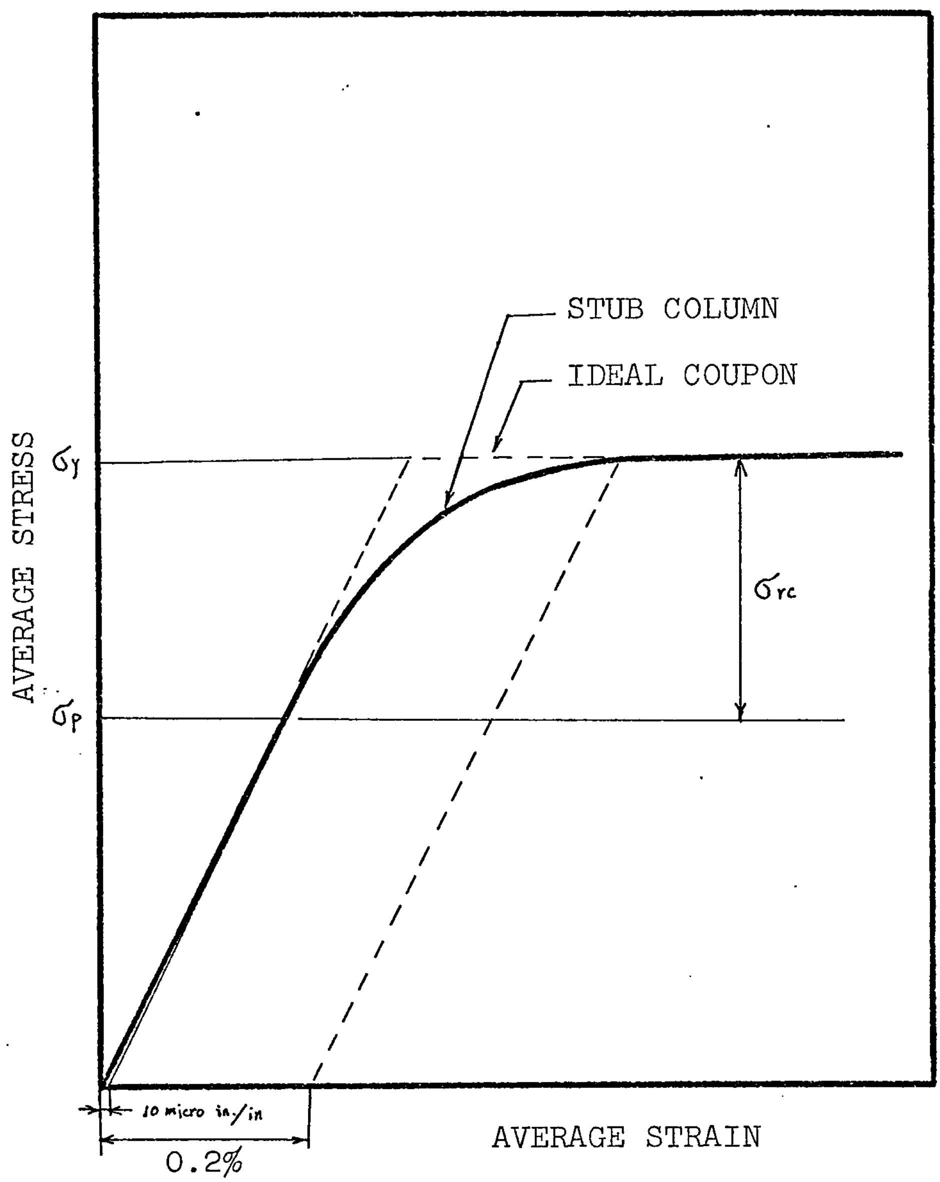

FIGURE 3

INFLUENCE OF RESIDUAL STRESS ON
STRESS-STRAIN CURVE

there may be accidental end eccentricity and this will affect the column strength. Bleich has introduced the concept of a practical method of designing eccentrically or laterally loaded columns.[11]

He introduces the ratio

$$\beta = \frac{\sigma_{co}}{\sigma_{cr}} \tag{3.2}$$

in which σ_{co} = the critical stress of the axially loaded column, and σ_{cr} = the critical stress of the eccentrically loaded column. This expression can be converted by

$$\sigma_{cr} = \frac{\sigma_{co}}{\beta} \tag{3.3}$$

where σ_{co} now is already obtained with the Euler load.

For the calculation of β values, the following formulas were developed for mild steel (σ_y = 34 and 40 kips/in^2) and for high-tensile carbon steel (σ_y = 50 kips/in^2):

Structural Steel (σ_y = 34 kips/in^2):

For L/r = 20 to 80: $\beta = (1 + \frac{k}{2}) + \frac{\sqrt{k}}{10{,}000}(\frac{L}{r})^2$

For L/r = 100 to 200: $\beta = 1 + \frac{12{,}200\sqrt[3]{k^2}}{(L/r)^2}$ (3.4)

For values $80 < L/r < 100$ interpolate linearly between β_{80} and β_{100}.

Structural Steel (σ_y = 40 kips/in^2):

For L/r = 20 to 75: $\beta = (1 + \frac{k}{2}) + \frac{\sqrt{k}}{9{,}000}(\frac{L}{r})^2$

For L/r = 95 to 200: $\beta = 1 + \frac{10{,}600\sqrt[3]{k^2}}{(L/r)^2}$ (3.5)

For values $75 < L/r < 95$ interpolate linearly between β_{75} and β_{95}.

High-Tensile Carbon Steel (σ_y = 50 kips/in^2):

$$\text{For } L/r = 20 \text{ to } 70: \quad \beta = (1 + \frac{k}{2}) + \frac{\sqrt{k}}{7{,}000}(\frac{L}{r})^2$$

$$\text{For } L/r = 90 \text{ to } 200: \quad \beta = 1 + \frac{8{,}400\sqrt[3]{k^2}}{(L/r)^2} \tag{3.6}$$

For values $70 < L/r < 90$ interpolate linearly between β_{70} and β_{90}.

The expressions (3.4) to (3.6) make it possible to compute β directly from given values of $k = e/r$ and L/r in case of rectangular cross-sectional shape.

The critical load for the column with accidental eccentricity can be calculated by Equation (3.3) after calculating the β-values.

Assuming the eccentricities ranging from e = 0.1 inch to e = 0.7 inch, values are calculated for the X-shaped column with Equation (3.6) for the high tensile carbon steel (σ_y = 50 ksi), as shown in Table IV. The β curves are presented in Figure 4.

The column strengths as affected by the eccentricities and cross-sectional shapes are calculated in the following chapter.

III. CROSS-SECTIONAL SHAPE

The column strength is considerably influenced by the particular shape of the cross section. This was proved by Chwalla, Ježek, and Fritsche, according to Bleich's book which

TABLE IV

β-VALUES CALCULATED WITH EQUATION 3.6

	k=e/r r=1.3						
L/r	0.07 (e=0.1)	0.154 (e=0.2)	0.231 (e=0.3)	0.308 (e=0.4)	0.385 (e=0.5)	0.462 (e=0.6)	0.538 (e=0.7)
20	1.054	1.099	1.143	1.186	1.228	1.269	1.311
30	1.074	1.128	1.177	1.225	1.272	1.318	1.363
40	1.102	1.167	1.225	1.281	1.334	1.386	1.437
50	1.138	1.217	1.287	1.352	1.414	1.474	1.531
60	1.181	1.279	1.363	1.439	1.512	1.581	1.646
70	1.233	1.352	1.452	1.543	1.627	1.707	1.782
80	1.292	1.436	1.555	1.661	1.759	1.852	1.939
90	1.188	1.298	1.391	1.473	1.548	1.619	1.686
100	1.152	1.241	1.316	1.383	1.445	1.502	1.556
110	1.126	1.199	1.261	1.317	1.367	1.415	1.459
120	1.106	1.168	1.219	1.266	1.310	1.348	1.386
130	1.089	1.143	1.187	1.227	1.263	1.297	1.329
140	1.078	1.010	1.007	1.196	1.227	1.256	1.284

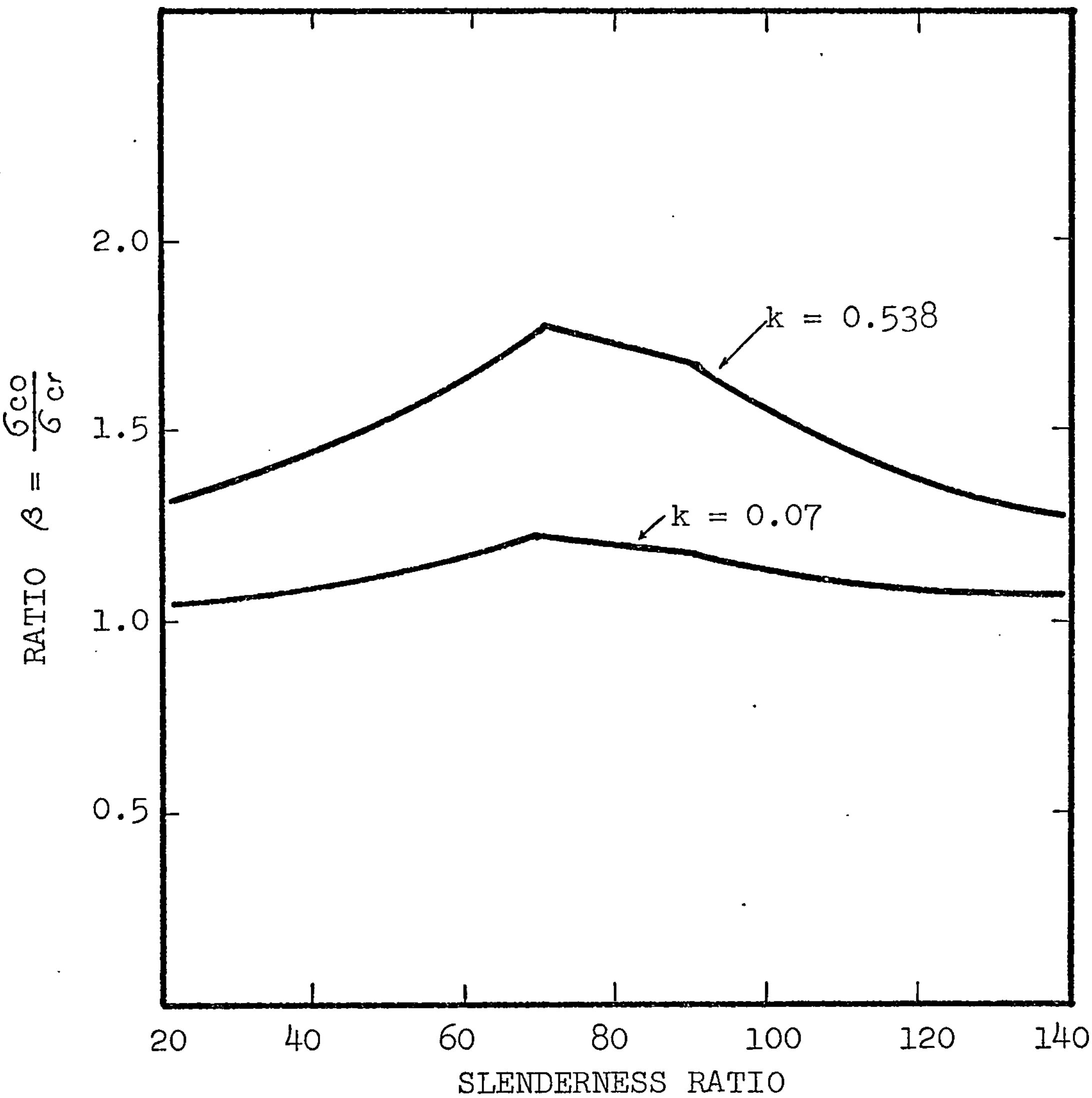

FIGURE 4

β -VALUE CURVES
(Equation 3.6)

summarizes as follows:

> As a rule, cross sections having the material concentrated near the center of gravity (i.e., + sections) possess greater strength, for a given L/r, than those where the material is located some distance from the center of gravity (H-sections for buckling in the plane of the web). The rectangular section lies between these extremes.[12]

The shape of the cross section related with the eccentricity e is shown in Table V giving the corresponding multiplier μ which depends upon the geometric form of the cross section.

Bleich has shown the effect of the shape of the cross section by the theory of the reduced modulus (Er). Figure 5 shows the variation of the column strength σcr with respect to Er/E when the material behaves by the stress-strain curve with an elastic limit of 29.2 kips/in^2 and with a yield point of 37.4 kips/in^2. The comparative strength between + and H sections is shown.[13]

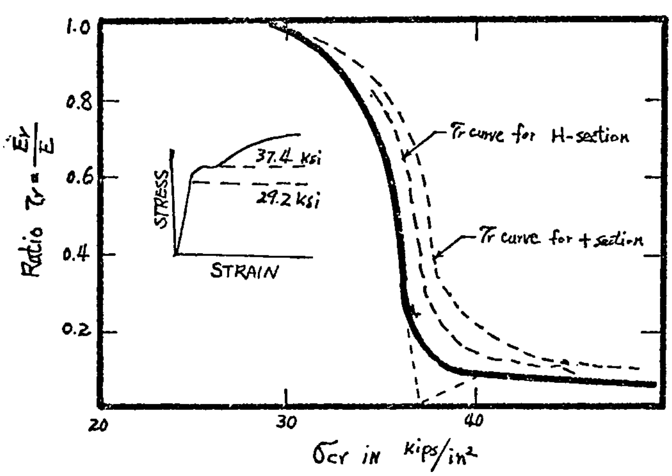

FIGURE 5

COMPARATIVE COLUMN STRENGTH CURVE BETWEEN + AND H SECTIONS[14]

TABLE V

FACTOR OF THE CROSS-SECTIONAL SHAPE[15]

Shape of Cross Section		μ
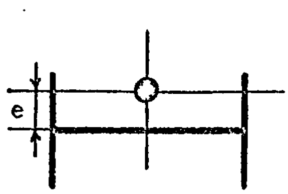	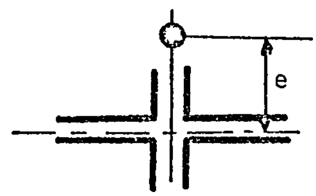	0.75
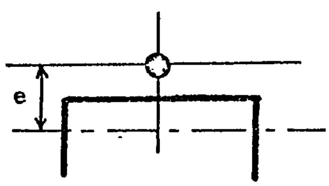	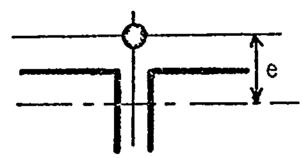	0.80
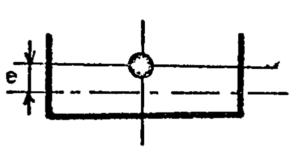	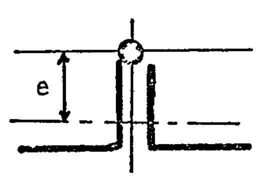	1.0
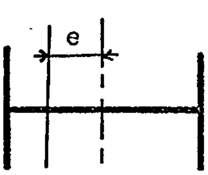	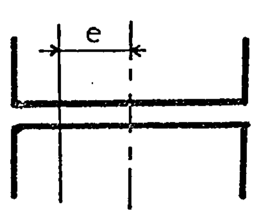	1.3

CHAPTER IV

THE COLUMN STRENGTH CURVE

It would be reasonable to discuss now the calculation of column strength, taking into consideration the factors affecting column strength as discussed in the previous chapter. This chapter deals with the calculations of column strength, using theoretical and empirical equations which are well known.

I. EULER'S CURVE

The Euler's buckling load is fully discussed in Chapter II. Taking into consideration the effects of residual stresses, eccentricity, and cross-sectional shapes, the final column strengths are shown in Figure 6, page 31. The purely theoretical column strength is shown with the Euler curve in the elastic range and the Bleich curve in the inelastic range. These curves form the upper bound curve and the actual column strength cannot exceed these lines. Table VI is the calculated values of the Euler stress, using Equation (2.2), taking the slenderness ratio between 20 and 125.

II. BLEICH'S CURVE

<u>With the Effect of Residual Stress</u>

Bleich proposes the following parabolic column strength curve for steel in the inelastic range:

TABLE VI

CALCULATED EULER FORMULA STRESS*
($E = 29 \times 10^6$)

KL/r	σ_{cr} (ksi)	KL/r	σ_{cr} (ksi)
20	715.55	75	50.88
25	457.95	80	44.72
30	318.02	85	39.61
35	233.65	90	35.34
40	178.89	95	31.71
45	141.34	100	28.62
50	114.49	105	25.96
55	94.62	110	23.65
60	79.51	115	21.64
65	67.74	120	19.88
70	58.41	125	18.32

*Directly indicative of column strength only when stress is less than the proportional limit.

$$\sigma cr = \sigma y - \frac{\sigma p}{\pi^2 E}(\sigma y - \sigma p)\left(\frac{KL}{r}\right)^2 \tag{4.1}$$

Equation (4.1) is not suitable if $\sigma p < 0.5\ \sigma y$, in which case erroneous strength values greater than the Euler buckling stress would be predicted for a certain range of KL/r values.

Since the departure from linearity in the effective stress-strain curve for a steel column is explained by residual stress, Equation (3.1), $\sigma p = \sigma y - \sigma rc$, can be substituted in Equation (4.1) and the following result is then obtained for $\sigma rc < 0.5\ \sigma y$:

$$\sigma cr = \sigma y - \frac{\sigma rc}{\pi^2 E}(\sigma y - \sigma rc)\left(\frac{KL}{r}\right)^2 \tag{4.2}$$

Thus, for $\sigma rc = 0.5\ \sigma y$

$$\sigma cr = \sigma y - \frac{\sigma y^2}{4\pi^2 E}\left(\frac{KL}{r}\right)^2 \tag{4.3}$$

Table VII shows the calculated values of Equation (4.3), taking the slenderness ratio from 20 to 130 of different structural steels.

With the Effect of End Eccentricity and Cross-Sectional Shape

The β ratio can be calculated with Equations (3.4) to (3.6) if the σy of the structural steel is well defined. The test specimens of X-shaped column have $\sigma y = 36$ ksi. With Euler buckling loads in Table VI, page 22, the column strength affected by the accidental end eccentricity and the cross-sectional shape can be calculated as described in Chapter III.

TABLE VII

CALCULATED COLUMN STRENGTHS IN THE INELASTIC RANGE WITH $\sigma_{rc} = 0.5\sigma_y$

	Steels with Yield Points of							
KL/r	33 ksi	36 ksi	42 ksi	50 ksi	60 ksi	70 ksi	80 ksi	100 ksi
20	32.62	35.55	41.38	49.13	58.74	68.29	77.76	96.51
25	32.41	35.29	41.04	48.64	58.03	67.33	76.51	94.54
30	32.15	34.98	40.61	48.04	57.17	66.15	74.97	92.14
35	31.84	34.61	40.11	47.33	56.15	64.76	73.15	89.30
40	31.48	34.19	39.53	46.51	54.97	63.15	71.06	86.02
45	31.07	33.71	38.88	45.58	53.63	61.33	68.68	82.32
50	30.62	33.17	38.15	44.54	52.14	59.30	66.02	78.16
55	30.12	32.58	37.34	43.40	50.49	57.05	63.09	73.58
60	29.57	31.93	36.45	42.14	48.68	54.59	59.88	68.56
65	28.98	31.22	35.49	40.78	46.71	51.92	56.38	63.10
70	28.34	30.45	34.45	39.30	44.59	49.03	52.61	57.20
75	27.65	29.63	33.33	37.72	42.31	45.93	48.56	50.87
80	26.91	28.76	32.14	36.03	39.88	42.61	44.22	44.72
85	26.13	27.82	30.87	34.23	37.28	39.08	39.61	39.61
90	25.29	26.83	29.52	32.32	34.53	35.33	35.34	35.34
100	23.49	24.63	26.59	28.17	28.62	28.62	28.62	28.62
110	21.49	22.30	23.36	23.65	23.65	23.65	23.65	23.65
120	19.30	19.70	19.88	19.88	19.88	19.88	19.88	19.88

Table VIII shows the calculated values of β ratio of σy = 40 ksi structural steel (Equation 3.5). The eccentricity ratio k was multiplied by the multiplier μ = 0.75 to take into consideration the cruciform shape factor as shown in Table V, page 20. The radius of gyration, r, is the value of the X-shaped column specimen, and the eccentricities are chosen as e = 0.1, e = 0.5, and e = 1.0 inch arbitratily.

Table IX, page 27, contains the calculated column strengths of the A-36 structural steel in Table VII, page 24, divided by the corresponding β-values in Table VIII. Therefore, the values of Table IX are the cruciform column strengths influenced by the eccentricities of 0.1, 0.5, and 1.0 inch when the material of the column is A-36 structural steel.

III. ALLOWABLE STRESSES FOR COLUMN DESIGN

The factor of safety is to provide a reasonable margin for all indeterminable factors which are described in Table III, page 13. On the subject of allowable stress in axially loaded compression members, the AISC Specification[16] reads as follows:

> 1.5.1.3.1 On the cross section of axially loaded compression members when KL/r, the largest effective slenderness ratio of any unbraced segment as defined in Sec. 1.8, is less than Cc:

$$Fa = \frac{1 - [(KL/r)^2/2Cc^2]\, Fy}{F.S.} \quad \text{Formula (1)} \qquad (4.4)$$

TABLE VIII

β-VALUES CALCULATED WITH EQUATION 3.5

	$\mu k = \mu e/r$				$\mu k = \mu e/r$		
KL/r	e=0.1	e=0.5	e=1.0	KL/r	e=0.1	e=0.5	e=1.0
20	1.04	1.17	1.02	70	1.16	1.44	1.70
25	1.05	1.18	1.34	75	1.18	1.48	1.76
30	1.05	1.20	1.36	95	1.17	1.51	1.81
35	1.06	1.22	1.39	100	1.16	1.46	1.73
40	1.07	1.24	1.42	105	1.14	1.42	1.67
45	1.08	1.26	1.46	110	1.13	1.38	1.61
50	1.09	1.29	1.50	115	1.12	1.35	1.55
55	1.11	1.32	1.54	120	1.11	1.32	1.51
60	1.12	1.36	1.59	125	1.10	1.29	1.47
65	1.14	1.39	1.64				

TABLE IX

COLUMN STRENGTHS CALCULATED WITH EQUATION 3.3
CRUCIFORM SHAPE AND A-36 STEEL

	$\mu k = \mu e/r$ (μ=0.75, r=1.3)				$\mu k = \mu e/r$ (μ=0.75, r=1.3)		
KL/r	e=0.1	e=0.5	e=1.0	KL/r	e=0.1	e=0.5	e=1.0
20	34.18	30.38	26.93	70	26.25	21.14	17.91
25	33.61	29.91	26.34	75	25.11	20.02	16.83
30	33.31	29.15	25.72	95	22.03	17.07	14.24
35	32.65	28.37	24.90	100	21.27	16.90	14.26
40	31.95	27.57	24.08	105	20.63	16.56	14.08
45	31.21	26.75	23.09	110	19.73	16.15	13.85
50	30.43	25.71	22.11	115	18.77	15.57	13.56
55	29.35	24.68	21.16	120	17.74	14.92	13.04
60	28.51	23.45	20.82	125	16.64	14.19	12.45
65	27.39	22.46	19.03				

where

$$F.S. = \text{factor of safety} = \frac{5}{3} + \frac{3(KL/r)}{8Cc} - \frac{(KL/r)^3}{8Cc^3}$$

$$Cc = \sqrt{\frac{2\pi^2 E}{Fy}} \qquad (4.5)$$

1.5.1.3.2 On the cross section of axially loaded columns when KL/r exceeds Cc:

$$Fa = \frac{149{,}000{,}000}{(KL/r)^2} \qquad \text{Formula (2)} \qquad (4.6)$$

The commentary to the specification points out that "Formula (1) is found upon the basic column strength estimate suggested by the Column Research Council."[17]

The basic column strength was discussed in Chapters II and III, bringing out the Equation (2.2) in the elastic range and Equation (4.3) in the inelastic range, assuming $\sigma p = \sigma rc = 0.5\,\sigma y$. A varied factor of safety has been applied to the column strength estimate to obtain the allowable working stress.

For very short columns, the AISC factor-of-safety has been taken as equal to, or only slightly greater than, that required for members axially loaded in tension. For longer columns, approaching the Euler slenderness range, the AISC factor-of-safety is gradually increased 15 percent, resulting in good agreement with column strength based on the combined effect of nominal crookedness and residual stress. The AISC factor-of-safety increases with increasing KL/r and reaches a value of about 1.97 when the slenderness ratio falls in the range governed by the Euler formula.

The numerical values of allowable stresses for the various grades of steel used in building construction are calculated as shown in Table X, and the same values can be found in the appendix of the AISC Specification. The allowable stresses of the A-36 structural steel are plotted for the lower bound of the X-shaped column strength in Figure 6, page 31.

TABLE X

ALLOWABLE STRESSES (IN ksi) CALCULATED WITH AISC COLUMN FORMULA

	Steels with Yield Points of					Steels with Yield Points of			
KL/r	33 ksi	36 ksi	42 ksi	50 ksi	KL/r	33 ksi	36 ksi	42 ksi	50 ksi
5	19.62	21.39	24.94	29.66	105	11.83	12.33	13.08	13.53
10	19.41	21.16	24.63	29.26	110	11.27	11.67	12.19	12.34
15	19.18	20.89	24.29	28.80	115	10.69	10.99	11.28	11.29
20	18.93	20.60	23.92	28.30	120	10.09	10.28	10.37	10.37
25	18.66	20.28	23.51	27.75	125	9.47	9.55	9.56	9.56
30	18.36	19.94	23.06	27.15	130	8.83	8.84	8.84	8.84
35	18.05	19.58	22.59	26.51	135	8.19	8.19	8.19	8.19
40	17.71	19.19	22.08	25.83	140	7.62	7.62	7.62	7.62
45	17.36	18.78	21.55	25.11	145	7.10	7.10	7.10	7.10
50	16.99	18.35	20.99	24.35	150	6.64	6.64	6.64	6.64
55	16.60	17.90	20.40	23.55	155	6.62	6.62	6.62	6.62
60	16.20	17.43	19.79	22.72	160	5.83	5.83	5.83	5.83
65	15.78	16.94	19.14	21.85	165	5.49	5.49	5.49	5.49
70	15.34	16.43	18.48	20.94	170	5.17	5.17	5.17	5.17
75	14.89	15.90	17.78	19.99	175	4.88	4.88	4.88	4.88
80	14.42	15.36	17.06	19.01	180	4.61	4.61	4.61	4.61
85	13.93	14.79	16.32	17.99	185	4.36	4.36	4.36	4.36
90	13.43	14.20	15.55	16.94	190	4.14	4.14	4.14	4.14
95	12.92	13.60	14.75	15.84	195	3.93	3.93	3.93	3.93
100	12.38	12.98	13.93	14.71	200	3.73	3.73	3.73	3.73

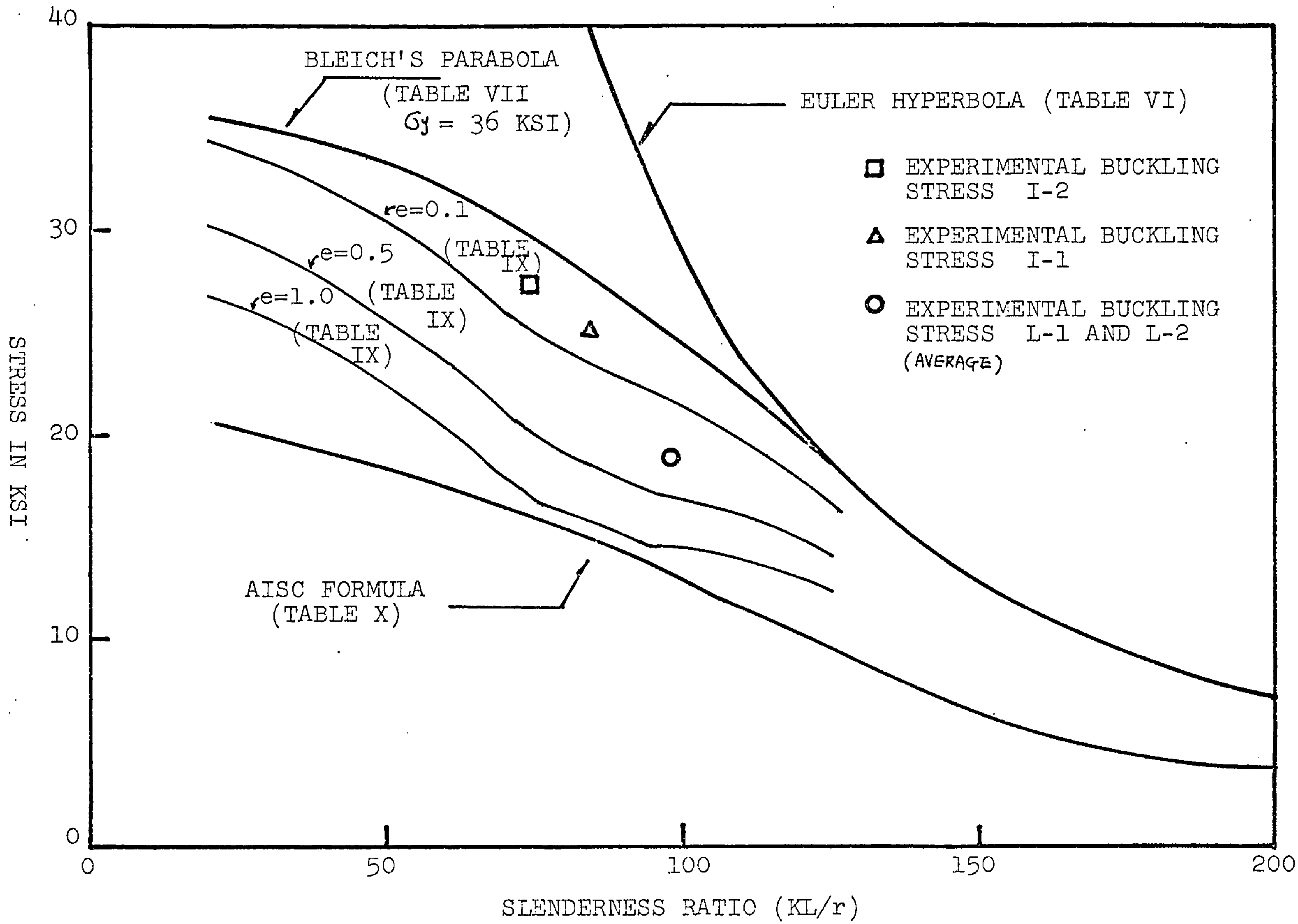

FIGURE 6

SUMMARY OF THE X-SHAPED COLUMN STRENGTH CURVES

CHAPTER V

EXPERIMENTS

The work reported here consisted of the testing of six columns. The two long columns were made of ASTM A-36 steel, and were provided by Mosher Steel Company. The other columns were made by cutting the end of the long column such that the intermediate length and the stub column tests might be possible. An outline of the test program is shown in Table XI where all of the experiments are listed with their specimen numbers.

TABLE XI

COLUMN TEST GENERAL

Material	Fabricated Number	L/r ratio	Specimen Designation	Test Purpose
A-36	1	98.1	L-1	Column Strength
	2	98.1	L-2	Column Strength
	3	83.2	I-1	Column Strength
	4	70.4	I-2	Column Strength
	5	13.8	S-1	Material Property
	6	13.8	S-2	Material Property

I. THE PRIMARY TEST PROCEDURE

Specimens

Since the major objective of the investigation was to check the theoretical column strength for centrally loaded columns, the primary tests were directed toward the determination of these quantities. The secondary tests were aimed to ascertain the quality of the material.

For the primary test, the specimen size was determined by the method of similitude, taking into consideration the limitation of the loading frame. Due to the availability of 1/2 inch by 1/2 inch rectangular bar and 3/16 inch plate, the ideal model cross section had to be slightly modified. Another important consideration in determining the test specimen was the slenderness ratio of the column. In order to keep the slenderness ratio up to 100, the column length was chosen to be approximately 129 inches. However, the L/r ratio of the actual test specimen came out as 98.1, with the column length of 127 inches. The dimensions of the test specimen are given in Figure 7.

Column-Test Apparatus

Loading frame. The column tests were carried out in the loading frame in the laboratory of the Civil Engineering Department. The loading frame is 12 feet long and is attached

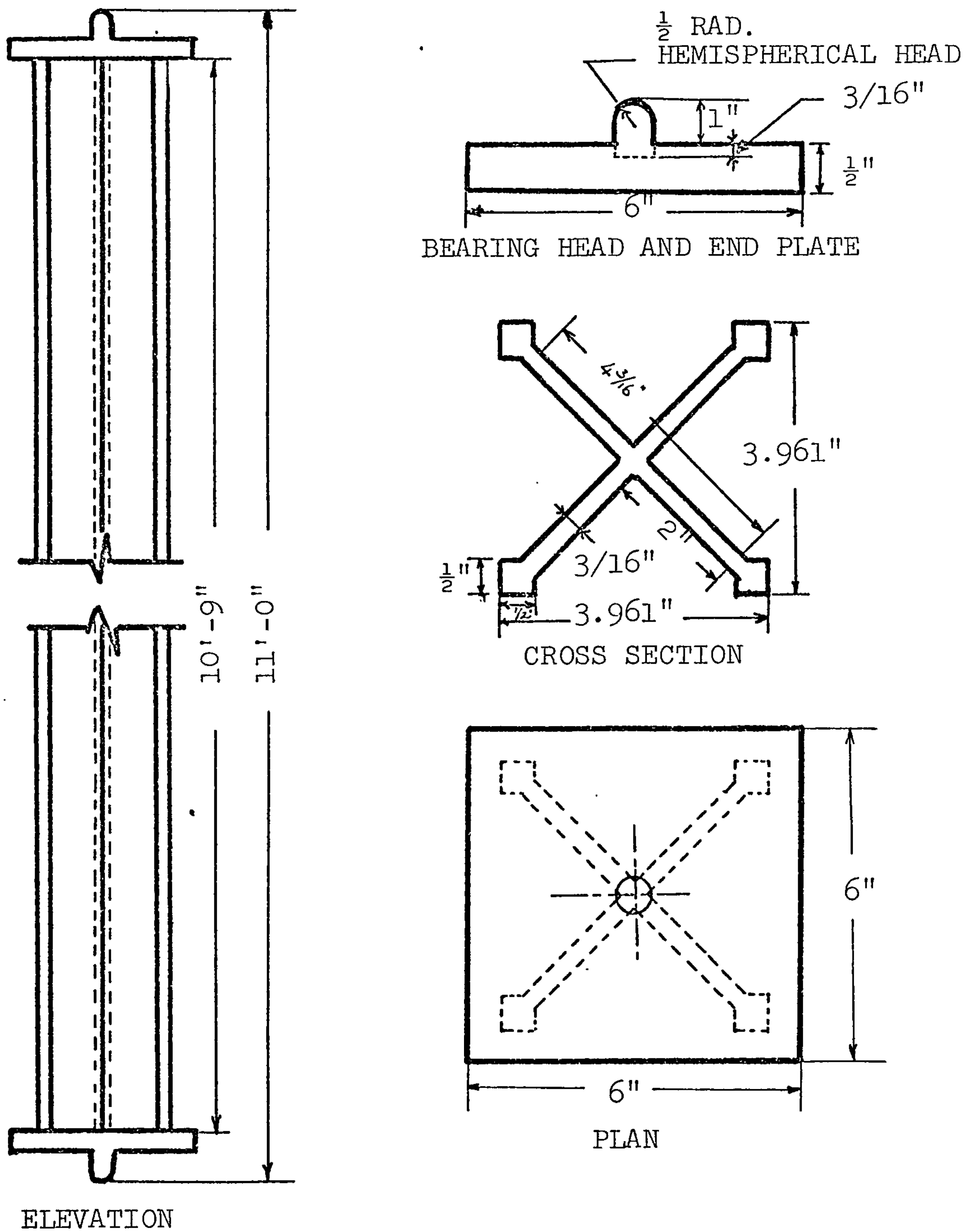

FIGURE 7

SPECIMEN DIMENSIONS FOR X-SHAPED COLUMN TEST to one of the 14WF34 columns of the laboratory. The maximum design capacity of the frame was 100,000 pounds. The general arrangement of the column test is shown in Figure 8, which is a photograph of an L-1 specimen positioned in the loading frame.

Load cell and hydraulic jack. The Model T-2550 load cell was used to measure the loads applied by the hydraulic jack. Both load cell and hydraulic jack were manufactured by Bayou Industries, Inc. The piston of the hydraulic jack was designed to extend 1.5 inches upward when the maximum load was applied. The minimum height of the load cell and hydraulic jack (14 inches) was taken into consideration in fabrication of the longest column test specimen.

Strain indicators. Two indicators were used in the experiment. The Budd Model P-350 indicator was connected to the load cell and the Bean Model 201 indicator was used to measure the strains of the column specimen. The Budd and the Bean indicators are self-contained, portable, compact, precision instruments. Due to the self-contained compensating gages, neither indicator requires that dummy gages be prepared, and both indicators make precise readings possible, due to the digital strain indicator.

The Budd indicator and the load cell were calibrated to obtain the converted values of the applied load in kips

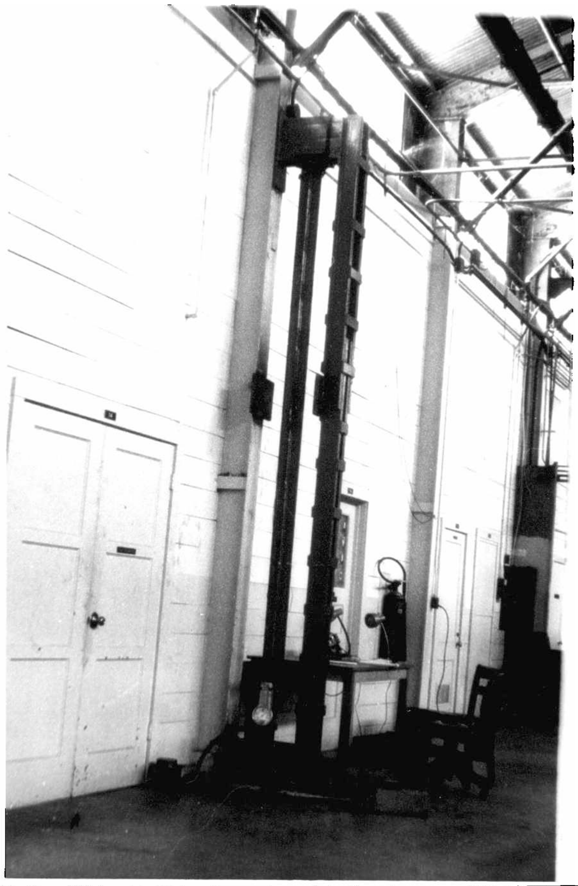

FIGURE 8

A PHOTOGRAPH OF L-1 SPECIMEN POSITIONED
IN THE LOADING FRAME

out of the digital strain readings in micro inch per inch. Table XII shows the calibration data of the Budd indicator and the load cell when the load cell was compressed by the universal testing machine.

TABLE XII

CALIBRATED DATA OF LOAD CELL AND BUDD STRAIN INDICATOR

Load (kips)	Strain (micro in/in)
5	132
10	241
20	508
40	1023
60	1532
80	2047
100	2566
120	3080
150	3840

Strain gages. SR-4 strain gages were attached at the midheight of the column. The gage type was AB-13, applicable in static and dynamic strain measurements. This gage is in a bakelite flat carrier which is 7/8 inch long and 11/32 inch wide. The resistance of the gage is 350 $\pm$ 8 ohms and the gage factor is 2.04 $\pm$ 1 percent. These data of the gage were considered in calibration of the Bean indicator.

<u>End fitting</u>. To obtain the desired boundary condition of the pinned end of the column specimens, the bearing head of the column end plate was fitted into the semi-circular hole of the end fitting plate of the column. These two end fittings were lubricated to eliminate the friction of the bearing head. The top end fitting plate was welded at the top center of the loading frame and provided the column the reference of the vertical alignment. The bottom end fitting plate was movable and supported by the load cell and hydraulic jack beneath.

<u>Transits and antennae</u>. Two transits were used to align the column in the loading frame. The end eccentricities were reduced as much as possible by aligning the column with the transits in two directions at the same time. The vertical hair line of the telescope of the transits was aimed at the top portion of the column, which is not movable, and the deviations of the bottom portion of the column were adjusted by moving the bottom supports. After alignment of the column with the two transits, the scopes of the transits were directed to the midheight portion of the column so that any buckling of the column in testing could be checked by the transits.

In order to check the torsional buckling of the testing column specimens, the slender metal rods, which the author would like to call antennae, were attached at the shorter column specimens, I-1 and I-2. The antennae attached at the column specimens were pointing at the marked wall of the loading frame, and the lateral and/or torsional displacement of the column specimens were indicated by the attached antennae.

Test Set-up and Alignment

To set up the test column, first the top fixture was placed in position and the bottom height adjusted by placing the end fitting plate, the load cell, hydraulic jack, and several pieces of 1-inch plate beneath the end of the column.

A geometrical alignment of the column was made with the two transits which were located approximately 90 degrees apart. The vertical hair-line of the telescope was adjusted to the top end of the column, and the deviation out of the hair-line was adjusted by moving the bottom plates.

The next step was to load the column in increments up to a predetermined maximum alignment load. It was necessary that this load be less than the proportional limit of the column specimen to ensure that premature yielding of the cross section would not occur in the process of aligning the column. The proportional limit of the material was determined from the result of the stub column test.

A certain degree of judgement was required in determining the maximum alignment load. The value depended on the proportional limit of the cross section, the column maximum carrying capacity, and the degree of accuracy of the alignment.

The alignment was based on the four corner-mounted strain gages at midheight. The alignment was considered satisfactory if the deviation of any of the four corner gage readings did not exceed 5 percent of their average value at maximum alignment load.

The eccentricity of the alignment was minimized by using both the transits and the strain gages.

Testing

The test was started with an initial load of about 1/15 to 1/10 of the calculated ultimate load of the column. All of the SR-4 strain gages were adjusted for initial readings and these readings were recorded. Besides recording the data, it was necessary that a point-by-point plot of the load-deflection curve and the load-strain diagram be made as the testing proceeded. The load was applied in appropriate increments as determined by the load-strain curve. The plot of load versus strain at the midsection gave the value of the proportional limit and indicated the occurrence of yielding in the cross section. The nearness to impending yielding was observed.

The critical load of column buckling was observed when some of the load-strain curves were stabilized, and the readings were plotted, decreasing after such a stabilization. The load increments were applied until the changes of increasing-to-decreasing on the load-strain curves were observed.

In addition to the strain gages, the antennae--which are slender aluminum pointers--were attached on the midheight of the column. These antennae were used to check the angular deflection of the column, provided initial marking were made on the wall indicating the tip ends of the antennae (see Figure 9).

Results--Presentation of the Data

For each loading increment, deflection data were obtained from the midheight strain gages. The results of the test are tabulated and plotted on Tables XIII through XVI and Figures 10 through 13, pages 43 through 51.

During the test, a plot was made of the load and of the average of the four strain readings. This plot was compared with the stub column test result to detect any unusual behavior of the column. The individual readings of the gages at the concave and convex sides and at the center line of the cross section are given. Also the stub column test results are shown for comparison. The plot may also be given as a stress-strain relationship by dividing each load by the actual measured cross-sectional area.

FIGURE 9

PHOTOGRAPH OF ANTENNAE ATTACHED ON THE COLUMN

TABLE XIII

DATA OF LOAD-STRAIN OBTAINED FROM L-1 SPECIMEN TEST

No.	Budd Reading $\mu\epsilon$	Calibrated Load kips	SR-4 Gage #1 $\mu\epsilon$	Gage #2 $\mu\epsilon$	Gage #3 $\mu\epsilon$	Gage #4 $\mu\epsilon$
1	55	2.15	0	0	0	0
2	186	7.27	35	58.4	64	70
3	343	13.40	108	128.5	140	170
4	472	18.42	161	196	198	250
5	575	22.42	196	242	248	307
6	679	26.42	231	289	303	362
7	785	30.70	274	345	353	431
8	891	34.80	304	397	409	505
9	996	38.90	333	447	475	571
10	1,097	42.80	356	502	530	642
11	1,195	46.70	374	531	564	710
12	1,301	50.90	380	572	646	781
13	1,404	54.90	362	610	780	850
14	1,450	56.50	350	625	860	885
15	1,492	58.40	321	628	961	892

$\mu\epsilon$: micro inches per inch

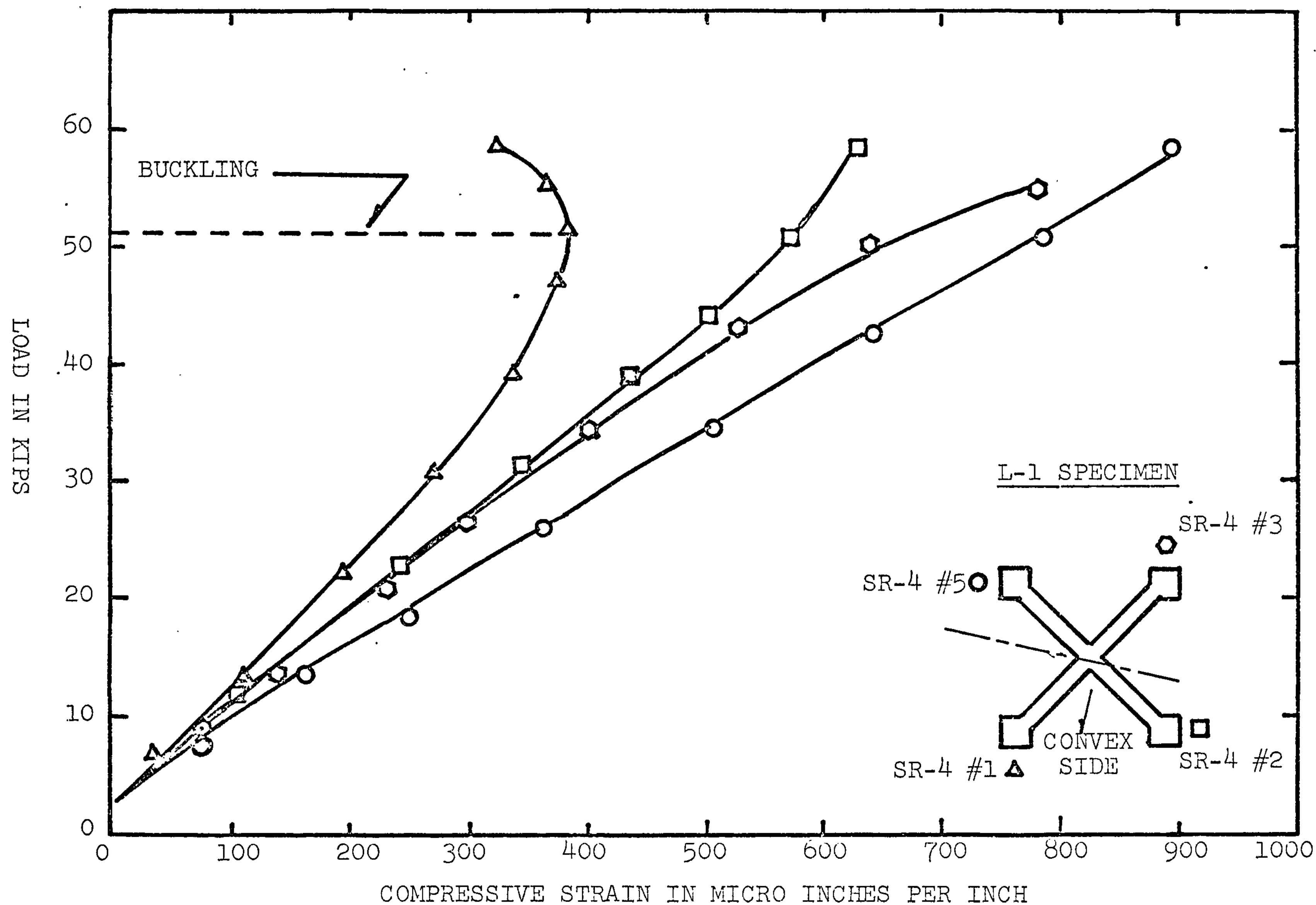

FIGURE 10

LOAD-STRAIN CURVES OF SPECIMEN L-1

TABLE XIV

DATA OF LOAD-STRAIN OBTAINED FROM L-2 SPECIMEN TEST

No.	Loads (kips)	SR-4 #1 $\mu\epsilon$	SR-4 #2 $\mu\epsilon$	SR-4 #3 $\mu\epsilon$	SR-4 #4 $\mu\epsilon$	SR-4 #5 $\mu\epsilon$	SR-4 #6 $\mu\epsilon$	SR-4 #7 $\mu\epsilon$	SR-4 #8 $\mu\epsilon$
1	0	0	0	0	0	0	0	0	0
2	9.3	105	97	126	104	103	143	102	100
3	18.2	178	172	245	219	219	298	190	210
4	27.2	260	242	368	304	438	458	289	315
5	32.2	290	269	435	371	532	555	339	374
6	37.0	321	298	505	430	630	650	394	429
7	41.6	336	313	560	496	730	756	438	479
8	46.3	348	324	630	555	840	875	494	537
9	51.0	339	321	719	629	990	1021	520	590
10	55.6	320	295	790	686	1130	1170	561	634
11	60.4	225	213	860	790	1330	1171	504	650

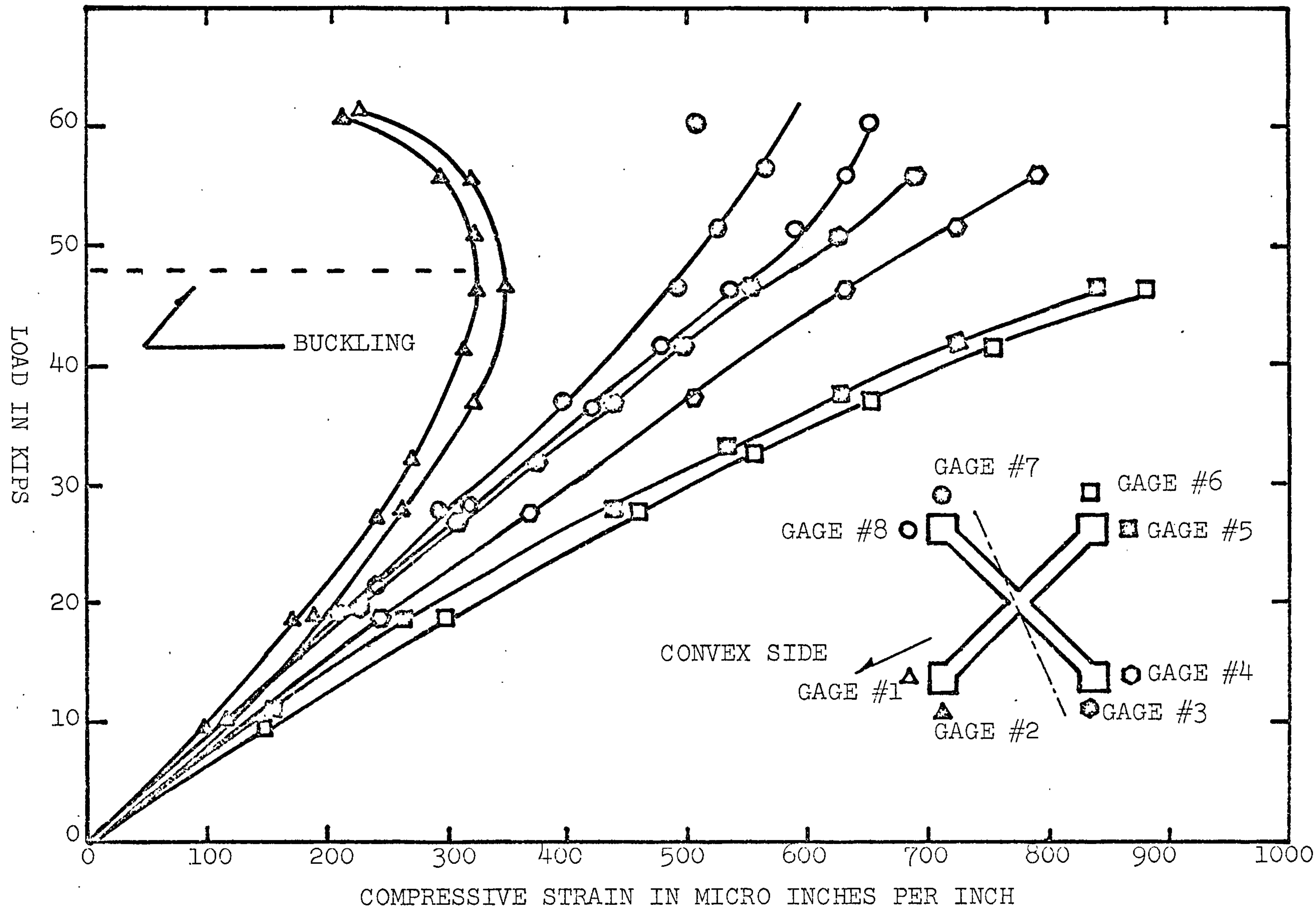

FIGURE 11

LOAD-STRAIN CURVES OF THE SPECIMEN L-2

TABLE XV

DATA OF LOAD-STRAIN OBTAINED FROM
I-1 SPECIMEN TEST

Applied Loads (kips)	SR-4 #1 $\mu\epsilon$	SR-4 #2 $\mu\epsilon$	SR-4 #3 $\mu\epsilon$	SR-4 #4 $\mu\epsilon$	SR-4 #5 $\mu\epsilon$	SR-4 #6 $\mu\epsilon$	SR-4 #7 $\mu\epsilon$	SR-4 #8 $\mu\epsilon$
0	0	0	0	0	0	0	0	0
11.1	85	88	125	114	123	96	87	125
16.5	146	140	198	175	192	146	131	174
18.2	161	154	199	201	221	175	160	213
18.7	172	160	200	204	222	181	160	219
20.5	181	166	201	219	245	198	175	242
22.2	201	193	204	242	265	210	188	260
24.2	213	201	230	268	290	242	204	289
26.4	230	219	268	298	318	263	219	315
28.5	248	233	475	321	321	268	245	347
32.5	292	274	498	373	376	310	274	397
37.8	320	318	576	446	446	362	347	475
43.0	380	365	645	522	520	402	356	542
45.0	394	376	710	542	542	426	365	574
47.0	410	394	730	571	570	444	400	591
50.8	440	420	790	628	620	475	431	688
54.7	472	458	845	685	680	502	458	740

TABLE XV (Continued)

Applied Loads (kips)	SR-4 #1 $\mu\epsilon$	SR-4 #2 $\mu\epsilon$	SR-4 #3 $\mu\epsilon$	SR-4 #4 $\mu\epsilon$	SR-4 #5 $\mu\epsilon$	SR-4 #6 $\mu\epsilon$	SR-4 #7 $\mu\epsilon$	SR-4 #8 $\mu\epsilon$
58.6	496	490	920	752	730	528	466	795
62.5	525	520	990	825	781	534	496	841
66.4	560	558	1160	900	835	540	536	898
70.4	578	580	1260	992	895	516	550	952
74.3	570	592	1390	1001	1010	476	566	1050
76.3	568	604	1480	1090	1090	440	566	1070
77.2	567	604	1560	1145	1120	415	570	1095
78.3	566	616	1590	1190	1150	381	566	1130
79.1	560	618	1640	1230	1180	360	560	1140

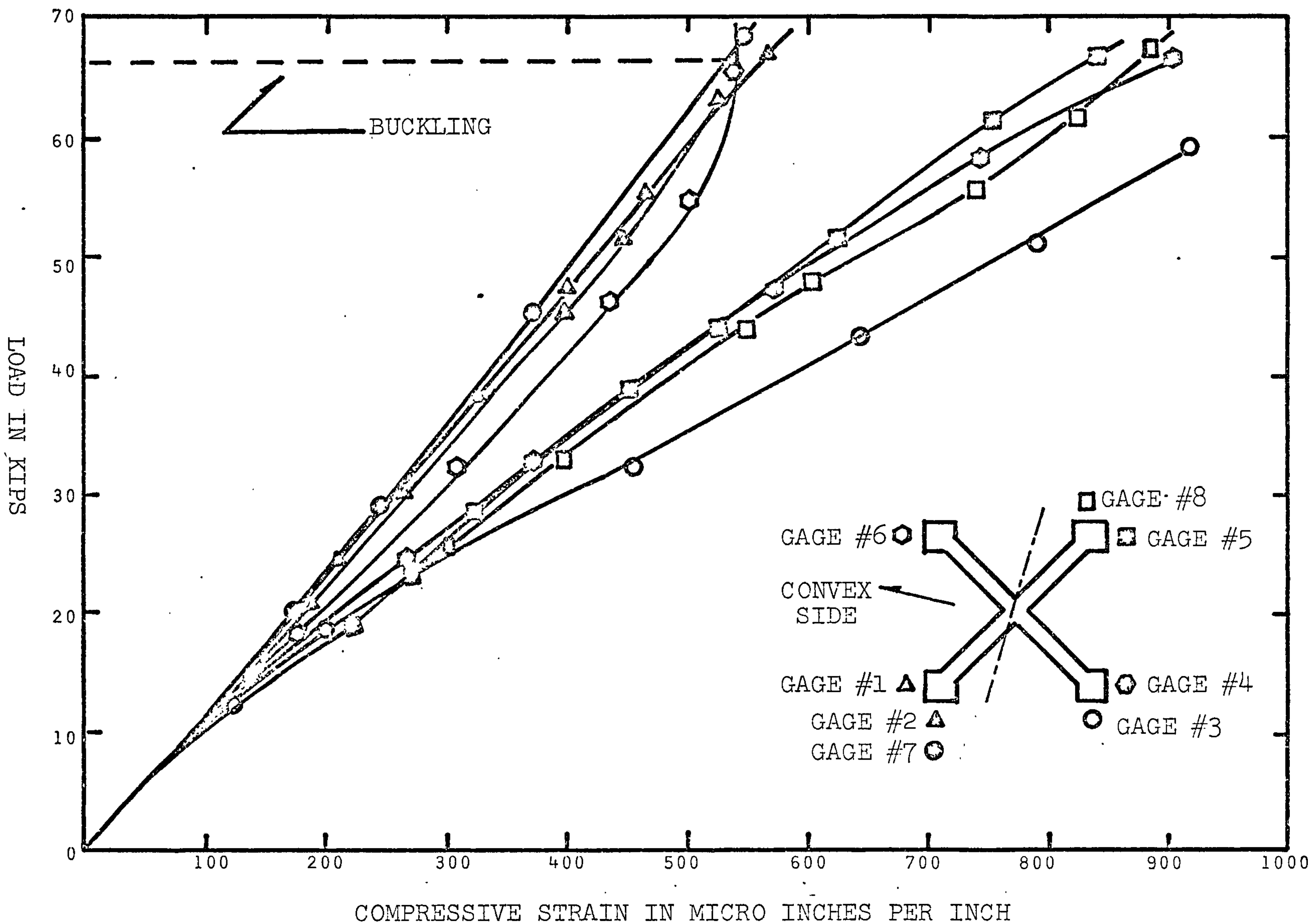

FIGURE 12

LOAD-STRAIN CURVES OF THE SPECIMEN I-1

TABLE XVI

DATA OF LOAD-STRAIN OBTAINED FROM I-2 SPECIMEN TEST

Loads (kips)	SR-4 #1 $\mu\epsilon$	SR-4 #2 $\mu\epsilon$	SR-4 #3 $\mu\epsilon$	SR-4 #4 $\mu\epsilon$
5	0	0	0	0
10	45	44	60	50
15	80	100	125	90
20	110	165	175	140
25	155	225	250	190
30	187	280	300	240
35	236	330	375	280
40	290	400	450	320
45	330	460	520	375
50	390	520	600	420
55	400	600	700	450
60	420	650	850	501
65	440	750	900	550
70	451	865	1025	575
75	450	1002	1100	600
80				

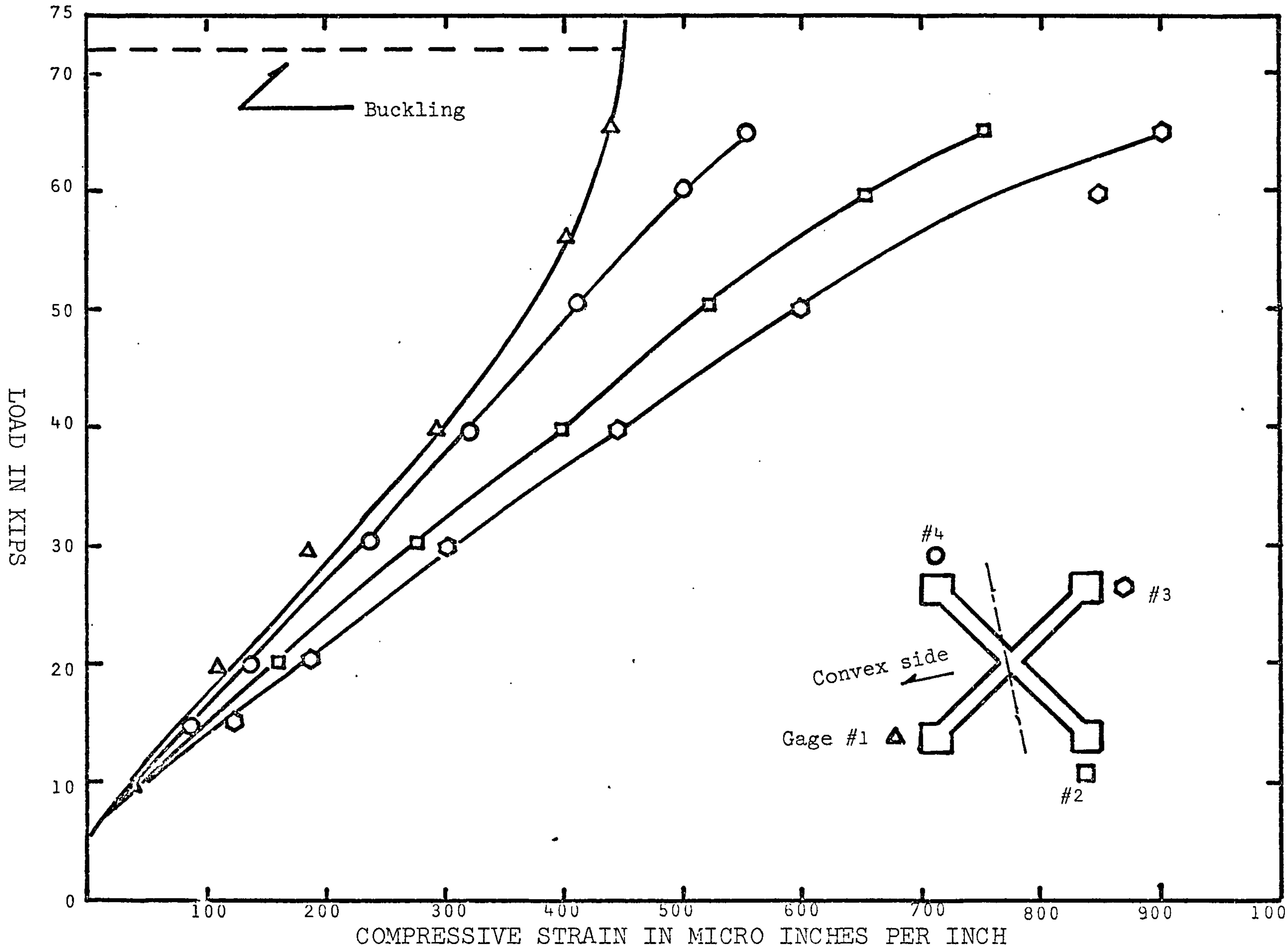

FIGURE 13

LOAD-STRAIN CURVES OF THE SPECIMEN I-2

Evaluation of Test Results

An evaluation of the results can be made by comparing the experimental value of the maximum load with the theoretical prediction. Table XVII shows the comparative data, and these data are plotted on Figure 6, page 31.

TABLE XVII

COMPARISON OF THEORETICAL AND EXPERIMENTAL BUCKLING STRESS

Specimens	Theoretical Buckling Upper Limit Stress in ksi	Theoretical Buckling Lower Limit Stress in ksi	Experimental Buckling Observed Stress in ksi	Experimental Buckling Percent (Upper Limit)
L-1	25.1	13.1	19.4	22
L-2	25.1	13.1	18.3	27
I-1	28.1	14.9	25.1	10
I-2	30.4	16.4	27.4	11

During the tests no local buckling was observed to occur, and all of the columns buckled with the mode of a sine curve. No torsional buckling was observed in testing of specimens L-1, L-2, I-1, and I-2, whose slenderness ratios were all greater than 65. The torsional buckling was predicted when the slenderness ratio was less than 65, as shown in Figure 2 of Chapter II, page 10. As a result, the torsional buckling was observed in the stub-column test.

The data obtained from the experiments are plotted in Figure 6, page 31, in between the upper limit (Euler's curve) and lower limit (AISC curve). Due to the fact that the longer the column, the bigger the eccentricity involved in the column strength, the longest column (average of two tests) buckled at a load about half-way between the upper and lower boundary lines. When the slenderness ratio of the column was between 70 and 90, the reduction of the column strength was expected to be greatest due to the existence of the residual stresses, as discussed in Chapter III.

The specimens L-1 and L-2 buckled over 20 percent below the theoretical value. This may be due to accidental end eccentricity, to the residual stress, or to inaccuracies in manufacture of the long columns.

II. THE SECONDARY TEST PROCEDURE

Object

The material of the test specimens was ASTM A-36 steel. The test objective was to obtain the mechanical properties of the columns by stub column test.

A stub column is defined as a column whose length is sufficiently small to prevent failure as a column, but long enough to contain the same residual stress pattern that exists in the column itself.[18]

The tangent modulus and other properties may be determined from the stress-strain relationship of the stub column test. The object of the stub column test is to determine the average stress-strain relationship of the complete cross section by means of the stub column, where the quality of the material may be determined.

Specimen Preparation

The stub-column length should be cut a distance at least equal to the section depth away from frame-cut sections. The length of the stub column should be

2d + 10", or 2d + 25 cm, or 3d minimum,

20ry, or 5d maximum

where

d = depth of section

ry = radius of gyration about weak axis

as described in the Technical Memorandum No. 3 of the Column Research Council.[19]

X-shaped stub columns were cut 18 inches from the end of the long column, and the ends were milled flat and perpendicular to the longitudinal axis of the column. The thin aluminum plate was placed between the milled surface of the stub column and the bearing head of the Universal testing machine, which reduced the unbalanced distribution of the load to a large extent.

Gaging

SR-4 strain gages of the same type as used in the primary test were mounted at the midheight of the column. These gages were used for the measurement of the stress-strain relationship.

Set-Up

The specimen was positioned in the Universal testing machine so that it rested between flat bearing plates. These plates were thick enough to ensure a uniform distribution of load through the specimen.

Alignment was achieved, more or less, by the use of beveled bearing heads of the Universal testing machine, and proper use of the strain gages. A photograph of the stub column positioned in the Universal testing machine is shown in Figure 14, and a photograph of the stub column and the strain indicator in Figure 15.

Testing

It was necessary that the stress-strain curve be constructed from as many experimental points as possible. After the proportional limit, the load increments had to be reduced so that there were sufficient data points to delineate the knee of the stress-strain curve.

The proportional limit was marked by the beginning of the deviation of the stress-strain relationship from the linear behavior.

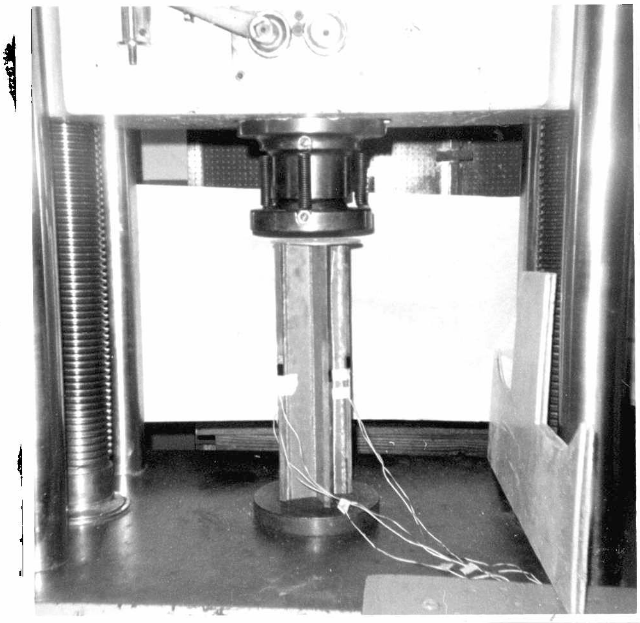

FIGURE 14

A PHOTOGRAPH OF STUB COLUMN POSITIONED IN THE UNIVERSAL TESTING MACHINE

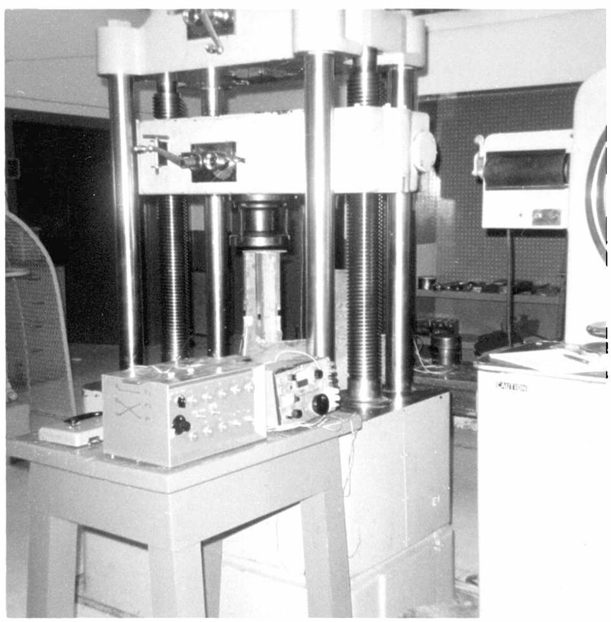

FIGURE 15

A PHOTOGRAPH OF STUB COLUMN AND THE STRAIN INDICATOR

The increments of strain obtained from the two stub column tests are shown in Tables XVIII and XIX, pages 58 and 59, and the respective average values are plotted in Figure 16, page 60.

Material Properties

The following information was obtained from the stress-strain relationship given by a stub-column compression test (S-1):

1. Young's modulus of elasticity: E

   $E = \frac{\Delta\sigma}{\Delta\epsilon} = 30 \times 10^6$

2. Proportional limit, σp, is the load corresponding to the strain above which the stress is no longer proportional to strain. It was best measured by the use of an offset of 10 micro in/in.

   $\sigma p = 20$ ksi

3. Yield strength is " . . . the stress, corresponding to the load which produces in a material, under the specified conditions of test, a specified limiting plastic strain."[20] An offset of 0.2 percent is suggested. The yield-stress level can be measured as 49 ksi, as shown in Figure 16. Since the material has the property of the minimum yield stress, $\sigma y = 36$ ksi, the yield stress measured from the stub column test should be greater than 36 ksi.

4. The residual stress can be determined from the data obtained from the stub column test. If the maximum yield point 49 ksi is taken, the residual stress is $\sigma rc = 29$ ksi. If the minimum yield point 36 ksi is taken, the residual stress is $\sigma rc = 16$ ksi.

5. The values of tangent modulus, Et, can be determined from the slopes of the knee curve line of the stress-strain diagram.

TABLE XVIII

DATA OF LOAD-STRAIN OBTAINED FROM S-1 SPECIMEN TEST

Load (kips)	Stress (Load/2.63) (ksi)	SR-4 #1 $\mu\epsilon$	SR-4 #2 $\mu\epsilon$	SR-4 #3 $\mu\epsilon$	SR-4 #5 $\mu\epsilon$	SR-4 #6 $\mu\epsilon$	Average $\mu\epsilon$	Accumulated $\mu\epsilon$
10	3.80	80	85	167	171	94	119.40	119.40
20	7.60	77	69	164	170	119	119.80	239.20
30	11.40	110	111	120	126	117	116.80	356.00
40	15.20	146	145	93	98	114	119.20	475.20
50	19.0	149	148	95	103	117	122.40	597.60
60	22.8	140	144	98	102	124	121.60	719.20
70	26.61	127	121	107	115	124	118.80	838.00
80	30.41	123	129	114	122	117	121.00	959.00
90	34.22	130	175	147	137	153	148.40	1107.40
100	38.02	149	202	196	71	172	158.00	1265.40
110	41.82	166	203	199	265	214	209.40	1474.80
120	45.62	158	292	467	154	204	255.00	1729.80
130	49.42	278	1987	657	1110	222	1050.8	2780.60

NOTE: Maximum load = 138 kips.

TABLE XIX

DATA OF LOAD-STRAIN OBTAINED FROM
S-2 SPECIMEN TEST

Load (kips)	Stress (Load/2.63) (ksi)	Gage #1 $\mu\epsilon$	Gage #2 $\mu\epsilon$	Accumulated Average
20	7.594	461	321	391
40	15.188	829	496	663
50	18.985	966	550	758
60	22.782	1,112	598	855
70	26.579	1,226	715	971
80	30.376	1,340	828	1,084
90	34.172	1,451	942	1,197
100	37.969	1,574	1,050	1,312
110	41.766	1,682	1,155	1,419
120	45.563	1,831	1,347	1,589
129	48.980	2,359	1,747	2,053
135	51.259	2,522	2,226	2,374
125	47.462	3,867	5,469	4,668

NOTE: Cross Section Area = 2.63 square inches.

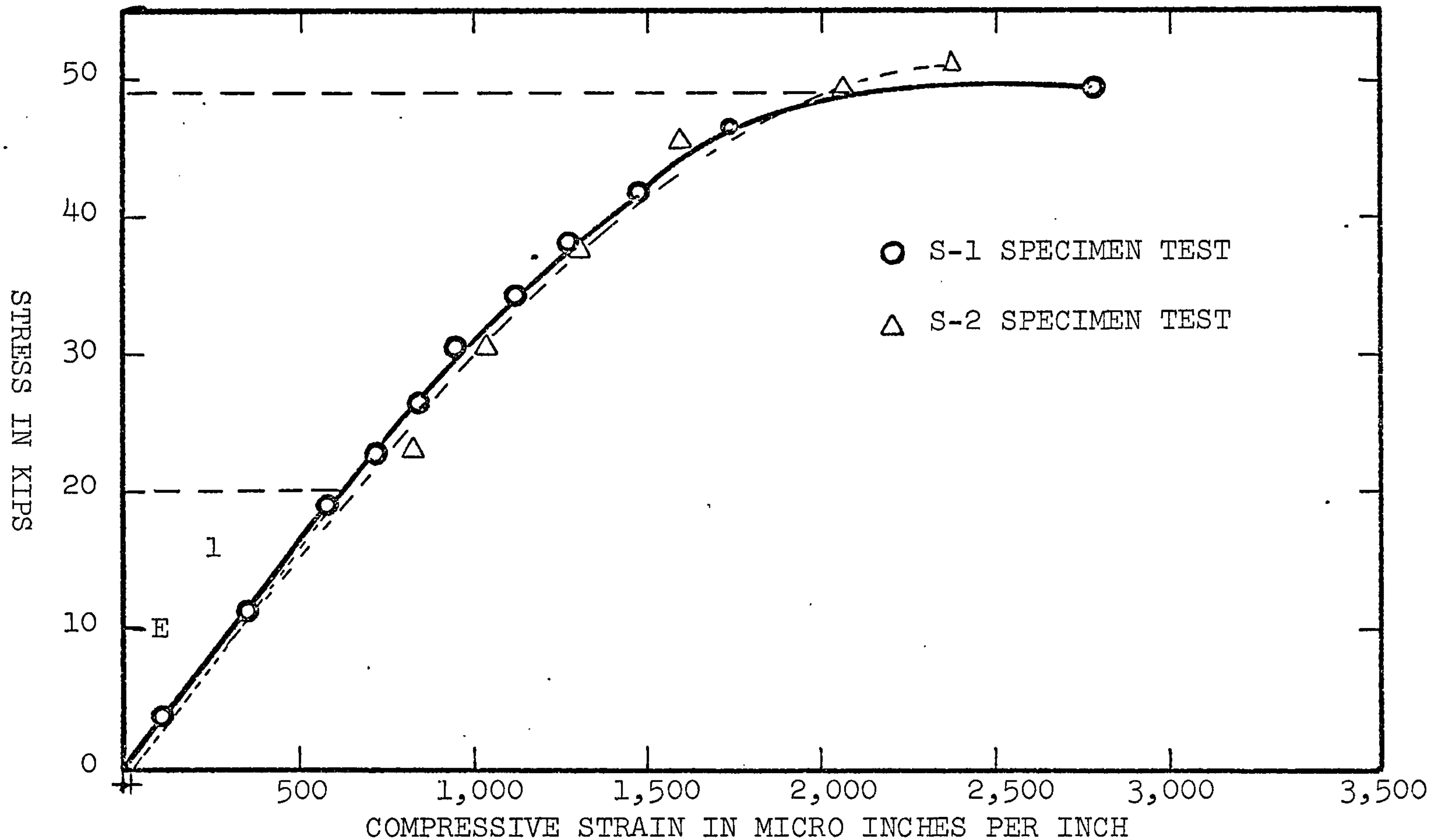

FIGURE 16

STRESS-STRAIN CURVE

CHAPTER VI

A COMPARISON WITH OTHER SHAPES

I. A COMPARISON WITH CRUCIFORM SHAPES

The cross sections having the material concentrated near the center of gravity possess greater strength for a given L/r than those where the material is located some distance from the center of gravity, according to F. Bleich.[21] The column strength of the cruciform sections (+ section) is known to be stronger than the column strength of the wide-flange sections for buckling in the plane of the web.

In Table IX, page 27, the column strengths are calculated taking into consideration the factor of the cross sectional shape ($\mu = 0.75$) and the eccentricities (e = 0.1, 0.5, and 1.0 inch). The cross-section was considered as the cruciform section, and the multiplier μ was taken from Table V, page 20. The column strength curves are drawn in between the upper and lower boundary lines in Figure 6, page 31. The column strength line of the cruciform section with the eccentricity e = 0.1 inch is taken as the reference line of the experimental X-shape column strength. Since the X-shaped cross section has the four rectangulars at the four tips of the cruciform section, the column strength of the X-shaped cross section influenced by the four rectangular stiffeners can be estimated by comparing the theoretical column strengths, taking into consideration the cruciform shape factor and the eccentricity with those of the experimental column strength of the X-shaped cross section. The eccentricity e = 0.1 inch is assumed to be an unavoidable value in the experiments.

The experimental column strengths, according to the slenderness ratio L/r = 98.1, 83.2, and 70.4, are plotted in Figure 6, page 31. The average buckling stress of the two experimental data of the long columns (L/r = 98.1) is plotted, and shows that the column strength of X-shaped section with L/r = 98.1 is weaker than that of the cruciform section with e = 0.1 inch, and stronger than that of the cruciform section with e = 0.5 inch. However, the column strengths of X-shaped section with L/r = 83.2 and 70.4 are plotted above the column strength curve line of the cruciform section with the e = 0.1 inch.

The column strength of the X-shaped section is estimated to be stronger than the cruciform section if the eccentricity e = 0.5 inch is assumed to be included in the test of L-1 and L-2 columns, and the eccentricity e = 0.1 inch is assumed to be included in the tests of I-1 and I-2 columns (see Table XX).

In general, the column strengths of the X-shaped cross section are estimated to be stronger than the cruciform section. The column strengths of the cruciform section when the column fails torsionally are not considered in this chapter, since the torsional buckling does not occur when L/r ratios are less than 65, as described in Chapter II.

TABLE XX

EXPERIMENTAL COLUMN STRENGTH COMPARED WITH CRUCIFORM COLUMN STRENGTH

	(1) Experimental Column Strengths of X-Shaped Section (ksi)	(2) Theoretical Column Strength of + Section (ksi)		(1)-(2) Difference of Column Strength (ksi)
		e=0.1	e=0.5	
L-1	19.1		16.97	+3.13
L-2	18.3		16.97	+1.33
I-1	25.1	23.88		+2.22
I-2	27.4	26.20		+1.20

II. A COMPARISON WITH WIDE-FLANGE SHAPES

Wide-flange shapes are often used as columns because of their low fabrication cost and ease of framing to other members. The wide-flange shape has been widely tested as a column and is the basis for most of the available data for basic column strength. Wide-flange shapes are widely used as columns because of the strong column strength in one direction.

As described in the previous section, F. Bleich has pointed out that the wide-flange section (H-section) is weaker than the cruciform section in buckling in the plane of the web for a given L/r, and the author has described that the X-shaped column strengths are stronger than the cruciform sections. Therefore, the X-shaped column strengths can be described to be stronger than wide-flange sections for a given L/r.

For further comparisons with wide-flange shapes, the allowable load for concentrically loaded columns in the AISC specifications is taken as a reference value of the X-shaped column strength. The concentric loads of the X-shaped section of Figure 1, page 2, are calculated with the Equations (4.4), (4.5), and (4.6), and the concentric loads of 12WF72 are taken from the AISC specifications, and the two concentric loads are compared in Table XXI. The allowable concentric loads of 8WF31 column strengths are compared also in Table XXI with the X-shaped cross section of Figure 17, page 67.

Table XXI shows that the allowable concentric loads of the X-shaped columns, taking into consideration the slightly less area than the wide-flange columns, are getting great. From the column length 18 feet, the values of the allowable concentric load are greater than that of 8WF31. The allowable concentric load of the 8WF31 column with the column length 15 feet, for instance, is 130 kips, while that of the

TABLE XXI

COMPARISON OF ALLOWABLE CONCENTRIC LOADS IN KIPS OF WF-SHAPE AND X-SHAPED COLUMNS CALCULATED WITH AISC FORMULA (A-36)

Nominal Depth and Width			12 X 12		8 X 8	
Column Shape			WF Shapes	X-Shapes	WF Shapes	X-Shapes
Weight per Foot			72	65	31	28
ASTM A-36	Effective length in feet KL with respect to least radius of gyration	6	431	399	178	167
		7	425	396	174	164
		8	420	392	169	162
		9	413	388	164	159
		10	407	384	159	156
		11	400	380	154	153
		12	393	377	148	150
		13	386	372	142	146
		14	378	368	136	143
		15	370	363	130	139
		16	362	358	123	136
		17	354	353	117	132
		18	345	348	110	128
		19	336	343	102	124
		20	327	337	95	120
		21	318	333	87	116
		22	308	327	79	111
		23	299	322	72	107
		24	288	316	66	102
		25	278	310	61	98
		26	268	302	57	93
		27	257	297	52	88
		28	245	291	49	83
		29	234	285	45	77
		30	222	277	42	72

TABLE XXI (Continued)

Nominal Depth and Width	12 X 12		8 X 8	
Column Shape	WF Shapes	X-Shapes	WF Shapes	X-Shapes
Weight per Foot	72	65	31	28
32	198	266	37	63
34	175	253		
36	156	236		
38	140	221		
40	127	206		
Properties				
Area A (in^2)	21.16	19.24	9.12	8.24
Ratio Yx/Yy	1.75	1.0	1.73	1.0
ry(in)	3.04	4.01	2.01	2.76

comparable X-shaped column is 139 kips. The difference of 9 kips between.the wide-flange and X-shaped column strengths may be considered to be strong in the X-shaped column.

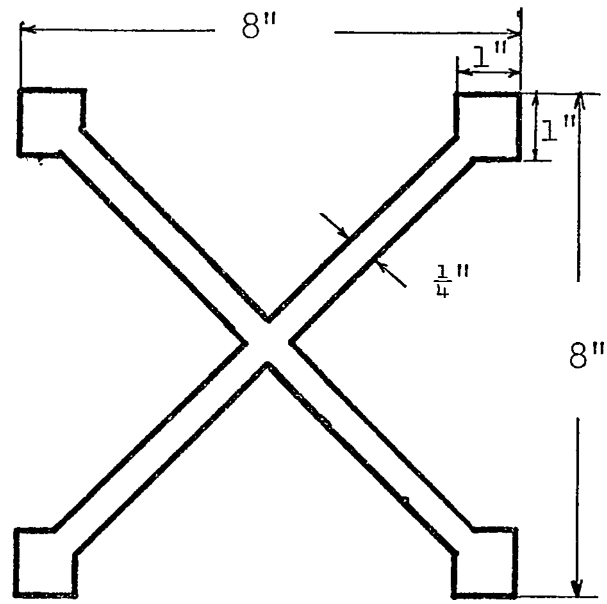

FIGURE 17

X-SHAPED COLUMN

Area = 8.242 in^2
Moment of inertia = 62.633 in^4
Radius of gyration = 21.76 in.

CHAPTER VII

CONCLUSION

The X-shaped column strengths are studied theoretically in Chapters II and III, and the calculations of the column strengths are plotted in Figure 6 of Chapter IV, page 31. Between the upper bound line of the Euler-Bleich curves and the lower bound line of the AISC curve, there are several curves drawn taking into consideration the influences of accidental end eccentricity and shape factor, as suggested by F. Bleich.[22]

The buckling strengths obtained from the primary tests are plotted in Figure 6 for the purpose of comparison with the theoretical values.

The material tests of the X-shaped column material show it to be ASTM A-36 steel.

By this series of tests, the author concludes that:

1. The X-shaped column is stronger than the cruciform section, which has no stiffeners on the four corners of the web. In Figure 6, the column strength curve of 0.1 inch eccentricity and + shape factor is drawn below the experimental X-shaped buckling stresses. Since 0.1 inch eccentricity is unavoidable in the experiments of the centrally loaded column test, the increased strengths above 0.1 inch eccentricity and + shape factor line are concluded to be the strengths, due to the rectangular stiffener at the four corners of the X-shaped column.

2. The centrally loaded long columns of X-shaped cross section buckle in the Euler buckling

mode and the shorter column lengths fail torsionally. During the test of compact and long columns, such as L-1, L-2, I-1, and I-2, torsional buckling was not observed except in the case of the stub-column tests, such as S-1 and S-2.

3. The X-shaped column is strong in local buckling due to the four stiffeners at the corners. No local buckling was observed during the tests.

4. The X-shaped column is equally strong in all directions. The direction of failure depends on the eccentricity at the end and fabricational error of the stiffeners. Test specimen L-2 failed at a lower buckling load because of poor fabrication of the column cross-section, especially one of the stiffeners. The column failed in the direction of the mal-fabricated flange.

5. Due to the equal strength in all directions of the X-shaped column, it is recommended to use the section for the central column of a building, monumental portion, and it may be advantageous for use as a pile.

6. It is recommended that in designing the X-shaped column, it would be permissible to use the AISC formula. The different sizes of the X-shaped cross-section are not devised in this thesis, but it is suggested that the increase of the radius of the gyration would not make the web thinner.

7. In this investigation, the effect of initial curvature was not considered because the test specimens were made without considerable initial bending. The initial curvature can have a great effect if the column is bent initially in the welding process.

8. The residual stress is observed to have a great effect on the column strength when the slenderness ratio is between 70 and 90. It is estimated that the lower buckling loads of L-1 and L-2 specimens were due to such residual stresses.

9. It was found that observing the column buckling phenomena with SR-4 strain gages was more effective than using the two transits and the antennae, because lateral displacements of the specimen during the test may occur and be observed through the telescopes due to the imperfect end supports. The antennae attached at the midheight of the column are useful to check the torsional buckling of the column.

In general, the X-shaped section can be proportioned to have as much strength as any other open cross section, and it does permit an easy connection with other members of the structure.

FOOTNOTES

FOOTNOTES

[1]F. E. Miller and H. A. Doeringsfeld, *Mechanics of Materials* (second edition; Scranton, Pa.: International Textbook Co., 1966), p. 2.

[2]J. B. Keller, "The Shape of the Strongest Column," *Arch. Rational Mech. Anal.*, V, No. 4 (1960), 275-85.

[3]S. P. Timoshenko and J. M. Gere, *Theory of Elastic Stability* (New York: McGraw-Hill Book Company, Inc., 1961), pp. 46-49.

[4]*Ibid.*, p. 180.

[5]R. Kappus, "Twisting Failure of Centrally Loaded Open-Section Columns in the Elastic Range," *NACA Technical Memorandum* No. 851, p. 2.

[6]A. Chajes and G. Winter, "Torsional-Flexural Buckling of Thin-Walled Members," *Proc. Am. Soc. Civil Engrs.*, ST (August, 1965), 120.

[7]S. P. Timoshenko, "Theory of Bending, Torsion and Buckling of Thin-Walled Members of Open Cross Section," *J. of the Franklin Institute*, CCXXXIX, No. 4 (April, 1945), 266.

[8]L. S. Beedle and L. Tall, "Basic Column Strength," *Trans. Am. Soc. Civil Engrs.*, LXXXVI (July, 1960), 139-73.

[9]Bruce G. Johnston (ed.), *Guide to Design Criteria for Metal Compression Members* (second edition; New York: John Wiley & Sons, Inc., 1966), p. 16.

[10]Beedle and Tall, *op. cit.*, p. 154.

[11]F. Bleich, *Buckling Strength of Metal Structures* (New York: McGraw Hill Book Company, Inc., 1952), pp. 41-45.

[12]*Ibid.*, p. 44.

[13]*Ibid.*, p. 13.

[14]*Ibid.*

[15]*Ibid.*, p. 45.

16 American Institute of Steel Construction, Inc., "Specification for the Design, Fabrication and Erection of Structural Steel for Buildings," _AISC Manual of Steel Construction_, Part 5 (sixth edition; New York: American Institute of Steel Construction, Inc., 1967), p. 5-16.

17 _Ibid._, p. 5-103.

18 Johnston, _op. cit._, p. 191.

19 _Ibid._, Appendix B.

20 _Ibid._

21 Bleich, _op. cit._, p. 44.

22 _Ibid._, p. 45.

BIBLIOGRAPHY

BIBLIOGRAPHY

American Institute of Steel Construction, Inc. "Specification for the Design, Fabrication and Erection of Structural Steel for Buildings," AISC Manual of Steel Construction. Sixth edition. New York: American Institute of Steel Construction, Inc., 1967.

American Society for Testing and Materials. Test Methods for Compression Members. Special Technical Publication No. 419. Philadelphia: American Society for Testing and Materials, 1967.

Beedle, L. S., and L. Tall. "Basic Column Strength," Trans. Am. Soc. Civil Engrs., LXXXVI (July, 1960), 139-73.

Bleich, F. Buckling Strength of Metal Structures. New York: McGraw-Hill Book Company, Inc., 1952.

Chajes, A., and G. Winter. "Torsional-Flexural Buckling of Thin-Walled Members," Proc. Am. Soc. Civil Engrs., ST (August, 1965), 120.

Johnston, Bruce G. (ed.). Guide to Design Criteria for Metal Compression Members. Second edition. New York: John Wiley & Sons, Inc., 1966.

Kappus, R. "Twisting Failure of Centrally Loaded Open-Section Columns in the Elastic Range," NACA Technical Memorandum No. 851, p. 2.

Keller, J. B. "The Shape of the Strongest Column," Arch. Rational Mech. Anal., V, No. 4 (1960), 275-85.

Miller, F. E., and H. A. Doeringsfeld. Mechanics of Materials. Second edition. Scranton, Pa.: International Textbook Co., 1966.

Roark, R. J. Formulas for Stress and Strain. Fourth edition. New York: McGraw-Hill Book Company, Inc., 1965.

Tall, L., and L. S. Beedle (eds.). Structural Steel Design. New York: The Ronald Press Co., 1964.

Timoshenko, S. P. "Theory of Bending, Torsion and Buckling of Thin-Walled Members of Open Cross Section," J. of the Franklin Institute, CCXXXIX, No. 4 (April, 1945), 266.

________, and J. M. Gere. Theory of Elastic Stability. New York: McGraw-Hill Book Company, Inc., 1961.